EXPERIMENTAL INVESTIGATION OF HYPERVELOCITY FLIGHT

By J. Lukasiewicz

Gas Dynamics Facility

ARO, Inc., Contract Operator, Arnold Engineering Development Center, Air Research and Development Command, United States Air Force

Summary—Experimental techniques which are being developed for investigation of hypervelocity flight are considered in relation to characteristics of trajectories of interest. A distinction is made between hypersonic and hypervelocity test facilities. Problems associated with the design of air heaters and hypersonic wind tunnel nozzles are discussed, with particular reference to axi-symmetric nozzles. The performance and limitations of shock tube tunnels, piston-compression tunnels, hotshot-type tunnels, aeroballistic ranges, and free flight are considered. The application of electric-arc method of heating air to drive wind tunnels (so-called hotshot type) and hypervelocity guns is discussed in some detail on the basis of experimental data available. The problems of simulating hypervelocity flight at low densities are discussed.

1. INTRODUCTION

At the close of the Second World War the construction of a 1×1 m (40×40 in.) hypersonic wind tunnel, with an upper Mach number limit of 10, was initiated by the German W.V.A. Supersonic Laboratory at Kochel[1].

It is significant that even today no such tunnel is in operation, at least in the Western Hemisphere. As a result, although in 1943 the flight of the V-2 rocket missiles could be adequately simulated in the wind tunnels then existing, the ground test facilities available today are inadequate in relation to the actual full-scale development of hypervelocity craft. This situation could be regarded as highly anomalous and large efforts are being made to improve it. The difficulties which were encountered in the development of hypersonic test facilities, the results achieved so far, and future developments are the subjects of this paper.

The review presented here is limited to experimental methods of investigation of aerodynamic, rather than structural, phenomena encountered in hypervelocity flight. For this reason, it is only concerned with air as the working medium.

2. PROBLEMS OF SIMULATION

Our knowledge, even in the engineering sense, of phenomena occurring in hypervelocity flight is, as yet, rather incomplete, whereas the practical difficulties of simulating them in ground-test facilities are obviously serious. We are thus confronted in the field of experimental investigation of

hypervelocity flight with these two questions: What are the realistic simulation requirements? What are the best techniques to meet them?

It seems likely that the answer to the first one will not come from theoretical studies alone, but rather that it will be obtained as a result of analysis of experiments in which different degrees of simulation will be achieved. This would indicate the necessity of developing a wide range of facilities—a course which, in fact, is presently pursued and which will eventually provide answers to the second question. Therefore, rather than state hypothetical simulation requirements in relation to various hypervelocity regimes and flow phenomena, we shall discuss briefly some of the characteristics of hypervelocity flows. Future experience, gained from problems encountered in the design and operation of hypervelocity spacecraft and from correlation of test data, will indicate the actual degree and range of usefulness of various types of simulation.

To obtain an indication of the ambient conditions likely to be encountered in hypervelocity flight, we shall first examine a few typical trajectories.

Some Typical Trajectories

The macroscopic hypervelocity phenomena in the earth's atmosphere cover a wide spectrum of velocity and altitude, the upper boundary belonging to meteorites which originate in the solar system and enter the atmosphere at a velocity of 236,000 ft/sec. However, we shall be here concerned with hypervelocity flight in a more restricted range, as determined by the particular types of trajectories which appear at the moment to be of engineering interest. Of these, the ballistic and boost-glide trajectories are most easily defined.

Extreme Ballistic Trajectories. From the point of view of aerodynamics, only the initial and final portions of ballistic trajectories might be of interest, since, even for short ranges, an optimum* trajectory reaches well above the dense atmosphere, to about one-quarter of the range.

As regards the initial, ascending portion of flight, it is found that because of effects of drag at low altitudes and of acceleration on structural weight, low accelerations, of the order of $2g$ or smaller, are favorable. Consequently, only relatively small velocities are developed within the atmosphere in this phase of flight.

The most serious aerodynamic effects occur on entering the atmosphere, during the final portion of flight. The motion then depends essentially on the velocity and angle of entry into the atmosphere and on the drag-inertia characteristics of the missile. We shall attempt here to define a ballistic trajectory which could be regarded as an extreme one; i.e. one which would exhibit maximum velocities at minimum altitudes.

When it is assumed that the drag coefficient is constant, the entry path straight and the density varies exponentially with altitude, then the

* Maximum range *in vacuo* for given initial velocity.

following relation holds for velocity in terms of altitude[2] during the final phase of flight:

$$= V/V_E = \exp -ke^{-\beta h}$$

where $k = C_D A \rho_{SL} g/(2\beta W \sin \theta_E)$

A = area on which C_D is based

h = altitude

V = velocity

V_E = velocity at entry

W = weight

θ_E = angle at entry to horizontal

ρ_{SL} = mass density at sea level

$\beta = 1/23{,}000\ \text{ft}^{-1}$

For the velocities considered and the altitude range in which deceleration takes place, the above is a good approximation.

The trajectory characteristics depend on the parameter k, whose physical significance can be appreciated by writing:

$$k = \frac{1}{2\beta \sin \theta_E} \frac{1}{l} C_D \frac{\rho_{SL}}{\delta}$$

where $W/g = \delta l A$, the missile mass, is expressed as a product of volume (lA) and average mass density δ. Thus, the value of k depends on

(i) θ_E or trajectory slope,

(ii) $1/l$ or scale factor, expressing the square-cube law,

(iii) drag coefficient C_D, and

(iv) relative average density δ/ρ_{SL}.

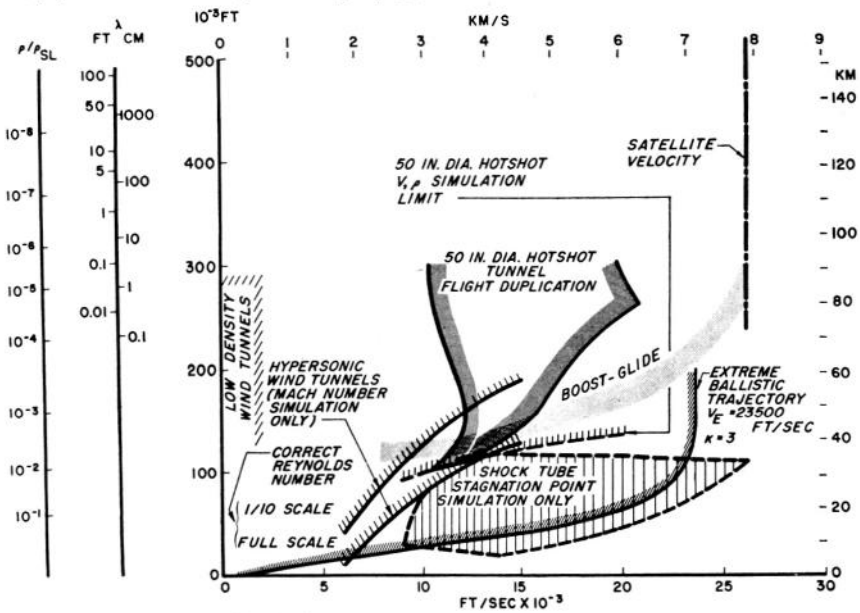

FIG. 1. Typical trajectories and regions of simulation.

Small values of k imply large velocities at low altitudes, and are obtained for large entry angles with large and dense missiles of low drag.

In order to determine the minimum value of k which might be of interest, several trajectories and missile shapes were considered. Values of k for conical (60° vertex angle) and spherical missiles, having a specific weight of 225 lb/ft^3 (one-half of the specific weight of steel), and weighing 2000 lb and 10,000 lb, and for trajectories with $\theta_E = 25°$ and 10° were calculated. A minimum value of $k \approx 3$ was thus obtained for a 10,000 lb conical missile.

The corresponding extreme trajectory, shown in Fig. 1,* was calculated for $V_E = 23{,}500$ ft/sec, which would give a 6000 mile range for an optimum trajectory ($\theta_E = 23{\cdot}3°$). For this trajectory, practically all of the deceleration takes places below 100,000 ft altitude.

Boost-glide Trajectories. Ideally, the so-called boost-glide trajectory consists of acceleration to a velocity such that, at the altitude of burnout, gliding flight at the chosen L/D ratio is possible and is continuously maintained, the altitude decreasing as the vehicle is retarded under the action of aerodynamic drag. Boost-glide trajectories[4], corresponding to $L/D \approx 5$ and wing loading of from 10 to 100 lb/ft^2, are indicated in Fig. 1 for all ranges (i.e. up to the satellite velocity). It will be noticed that, unlike in the case of the extreme ballistic trajectory, the hypervelocity region of the glide trajectories occurs at altitudes between 100,000 and 200,000 ft.

There is, of course, no upper altitude limit to hypervelocity trajectories of ballistic or orbiting type. However, at extreme altitudes, the interest would shift from aerodynamic phenomena to physical properties of space.

Dynamics of Trajectories. From the point of view of simulation requirements, the velocity-altitude spectrum of practical trajectories should be supplemented by consideration of dynamic characteristics of trajectories and vehicles in flight. The complex problem of the dynamic behavior of a vehicle whose velocity and altitude are rapidly changing could be investigated by determining separately the dynamic and the static model characteristics under steady flow conditions. However, a true trajectory simulation would be desirable for investigation of particularly unsteady trajectories and such phenomena as, for example, ablation cooling.

Certain types of hypervelocity trajectories involve very large time rates of variation of ambient density and velocity. For example, for the extreme ballistic trajectory here considered, the deceleration from 23,000 ft/sec at 100,000 ft altitude to about 1000 ft/sec at impact takes place in about 15 sec. The maximum deceleration of about 60 g (or about 2000 ft/sec^2) is experienced at an altitude of 40,000 ft and at a velocity of 14,000 ft/sec. This corresponds to a dynamic pressure variation of 240 atm/sec and to a total enthalpy variation of −240 CHU/lb sec. Simulation

* Throughout this paper the properties of atmosphere, as given in Ref. 3, were assumed.

of such large rates of pressure, temperature and velocity variation would be, of course, extremely difficult to achieve.

It has been pointed out by Allen[4] that dynamic stability of hypervelocity vehicles may present serious structural, cooling and guidance problems. ICBM types of vehicles may be expected to enter the atmosphere at attitudes far removed from equilibrium and to perform oscillations of varying amplitude and frequency. The same would be true of skip and boost-glide type spacecraft, if deviations from the design values of attitude, altitude, and velocity at burnout occurred.

There is no reason why standard techniques of dynamic stability testing should not be extended to hypersonic wind tunnels, although such tests have not been carried out so far. There are, however, serious difficulties in conducting dynamic tests in hypervelocity tunnel facilities, due to the short run times available. In this respect, free flight and hypervelocity range techniques may offer greater possibilities.

Real Gas Effects

Because of the high stagnation enthalpy levels in hypervelocity flight, the phenomena which are in general referred to as the "real gas effects" may influence appreciably the flow field. Also, the investigation of such complex processes as mass transfer cooling (e.g. film and oblation cooling) may actually require exact duplication of flight conditions. It may not be therefore possible to obtain realistic simulation by duplication of Mach and Reynolds numbers alone as is customary in supersonic flow, and it is for these reasons that we shall use the term *hypervelocity* as distinct from *hypersonic*, the latter being often associated with facilities in which only the Mach number is simulated.

We may immediately note the types of flow in which real gas effects are present. These are evidently restricted to the regions of high deceleration,* as a result of either compression or viscosity in the model field of flow. In other words, *inviscid* hypervelocity flows about *slender* configurations would be free from real gas effects and Mach number would be the only similarity parameter involved. Nevertheless, it is found that the types of flow which exhibit real gas effects are among the ones to be associated with hypervelocity craft. For example, blunt shapes are favorable in the critical aerodynamic heating areas, and heat transfer in general depends on the boundary layer flow. Moreover, Reynolds numbers at high altitudes are small and therefore viscous interactions can be pronounced.

The real gas effects become progressively larger as the total enthalpy of air is increased with the flight speed increasing.

Up to temperatures of about 600°K, corresponding to velocities of 3000 ft/sec or $M \approx 3$ in the stratosphere, the air can be regarded as a perfect gas. At higher velocities, the effects of vibration become apparent,

* Relative to a stationary model.

but no chemical changes take place. This region extends to about 2000°K, or 7000 ft/sec, corresponding to a Mach number of about 7.

The third range if characterized by chemical changes, namely the appearance of nitric oxide, atomic oxygen, and nitrogen, in this order. The amount of these components depends on enthalpy as well as on entropy of the air, and therefore, for exact simulation, the actual state of the air has to be duplicated.

In the upper region of the chemical range, at enthalpies corresponding to speeds of 20,000 ft/sec and greater, ionization becomes significant and large quantities of positively and negatively charged particles appear in the air, which increasingly resembles a plasma. The electrical conductivity increases to values comparable to and larger than that of sea water. Consequently, at near-escape velocities, interactions between magnetic and flow fields may be of practical interest. Also, radiation may become significant.

In the above brief outlines of the real gas effects we referred to the state of the air as determined by the total enthalpy of flow. Although these conditions correspond to maximum deviations from the perfect gas characteristics, they may not be necessarily significant in relation to flow about hypervelocity vehicles, and, to assess this, typical flow cases must be examined. We shall first consider the cases in which the Reynolds number is sufficiently large so that the interaction of inviscid and boundary-layer flow may be neglected.

For lifting type of hypervelocity vehicles with cooled walls, surface temperatures, except in the stagnation regions, would be appreciably smaller than the recovery temperature, the highest ones occurring within the boundary layer, away from the wall. As pointed out by Smelt[5], dissociation would not take place in the boundary layer and the region of vibration effects would be extended to speeds of the order of 10,000 ft/sec and higher. Calculations of oblique shocks for air in chemical equilibrium[6] indicate that for values of normal component of the Mach number of up to 4, only small deviations from perfect gas flow conditions ($\gamma = 1{\cdot}4$) occur, the density downstream of the oblique shock being affected by less than 10%, and the entropy rise being practically unaffected. For example, this would be true for a flow deflection of 10° at 10,000 ft/sec and 100,000 ft altitude, corresponding to a normal Mach number component of only 2·5.

More generally, it is found[7] that hypersonic similarity parameter $M_\infty \tau$ with τ = thickness ratio, is adequate in the case of air in equilibrium at values of $M_\infty \tau \leqslant 3$ about.

However, it is likely that, in order to reduce aerodynamic heating rates, hypervelocity vehicles will have relatively blunt wings and bodies. Conditions behind a normal shock provide a useful guide to the magnitude of real gas effects in the stagnation regions created by such shapes.

At enthalpies corresponding to vibrational imperfections, the deviations from the perfect gas characteristics consist essentially, at low densities, of an increase in the specific heats and the attendant reduction

of their ratio γ. However, at large densities, such as would be encountered in the stagnation regions at lower altitudes, the effects of intermolecular forces tend to counteract the vibrational deviations, resulting in an approximately perfect gas behavior.* For example, at altitudes between 50,000 and 100,000 ft and at 5000 ft/sec the value of γ behind a normal shock is about 1·33, whereas at 200,000 ft it is only 1·22. This would indicate that for flight at lower altitudes and at velocities in the range of vibrational imperfections, useful simulation, including the stagnation regions of flow, might be possible at lower than flight velocities.

At still larger enthalpies, chemical reactions take place and numbers of particles increase. The magnitude of these changes is indicated in

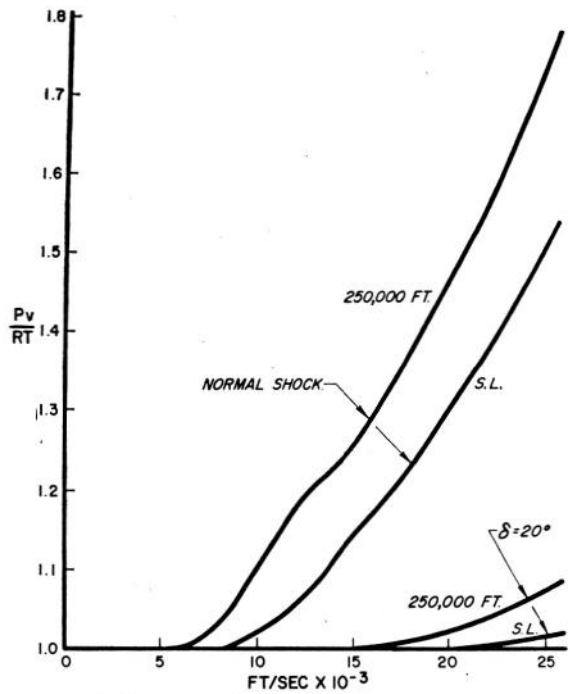

FIG. 2. Compressibility behind normal and oblique shock at sea level and 250,000 ft altitude[44].

Fig. 2 in which the value of Pv/RT, which can be regarded as a measure of dissociation, is plotted against velocity for conditions behind a normal and an oblique shock (flow deflection of 20°) at sea level and 250,000 ft altitude[44].

We shall note from this figure that in the stagnation region appreciable dissociation is present at 10,000 ft/sec and at high altitude (up to 10%), increasing up to 50% at 20,000 ft/sec. In fact, the dissociation of oxygen

* For this reason, expansions in hypersonic tunnel nozzles can be treated approximately as for a perfect gas[5].

is complete at about 15,000 ft/sec. The effect on γ is large, a value of about 1·13 corresponding to flight at 23,000 ft/sec at altitudes between 100,000 and 200,000 ft. On the other hand, the dissociation effects are small even at 25,000 ft/sec for small (20°) flow deflections.

Reynolds and Mach Numbers

It is known that heat transfer rates critically depend on the character of the boundary layer. As an example, at a Reynolds number of 10 million ($M = 10$ at 140,000 ft), a change from laminar to turbulent boundary layer is estimated[8] to cause a five-fold increase in the Stanton number. The phenomenon of boundary layer transition, so far in general inadequately understood, is thus particularly important in the hypervelocity flight regime and the advantage of close duplication of Reynolds number and ability to vary it over wide ranges is evident.

On the other hand, from the point of view of inviscid flow characteristics, the requirements for exact simulation of Mach number in general decrease with Mach number increasing. This is apparent, for example, from the rate of variation of pressure coefficient on slender bodies with Mach number, which is proportional to $(M_\infty - 1/M_\infty)^{-1}$.

In order to appreciate the relationship between the flow velocity, Mach and Reynolds numbers in facilities in which hypervelocities are obtained by isentropic expansion, it is instructive to consider the variation of the latter two parameters at constant reservoir conditions. For example, by varying the expansion ratio (or throat area) by a factor of 32 at 15,000 ft/sec flow velocity in the test section, the Reynolds number could be increased from its value at 200,000 ft altitude by a factor of 10, while the Mach number would be reduced from 14·3 to 7·15. The corresponding reduction in flow velocity would amount to less than 4%, due to the large ratio of total to static enthalpy, equal to 42 in this case.

More generally, the approximate relationship between Mach number, Reynolds number and expansion ratio, at constant flow velocity and assuming viscosity $\mu \propto T^{0.8}$, is given by:

$$Re_\infty \propto M_\infty^{-3.4}, \qquad M_\infty \propto (A_\infty/A^*)^{0.2}, \qquad Re_\infty \propto (A_\infty/A^*)^{-0.68}$$

Hence the ratio of the percentage variation of Mach and Reynolds numbers equals:

$$\frac{\mathrm{d}Re/Re}{\mathrm{d}M/M} \approx -3{\cdot}5$$

indicating that large changes in Reynolds number are obtained with relatively smaller changes in Mach number by varying the expansion ratio.

Effects of Decreasing Density

Equilibrium Flow. As already indicated, the velocity-altitude spectrum of hypervelocity trajectories may extend to regions of negligible density and large mean free path. Furthermore, the range of low densities corresponds to high velocities.

As the density is reduced, low Reynolds number effects would be expected to become appreciable when significant interaction between the boundary layer and inviscid flow occurs. This would cause, for example, effective blunting of bodies and hence an increase in pressure drag. The merging of the boundary layer with the shock wave in the stagnation region, as a result of thickening of the boundary layer, would be expected to occur[9] at a Reynolds number (based on the nose radius) of the order of $Re_\infty \approx M_\infty^2 \sqrt{r}$, where $r = \rho_2/\rho_1$ = density ratio across normal shock or at a Knudsen number (based on the nose radius) $Kn_\infty \approx 1/(M_\infty \sqrt{r})$. Thus, such effects would be significant at Reynolds numbers of the order of 1000 to 100.

At still smaller densities, the molecular flow effects would appear. In the past, following Tsien[10], it has been customary to distinguish between various low-density flow regimes on the basis of somewhat arbitrary assumptions as to the significance of the Knudsen number based on the ambient mean free path and a characteristic length, such as the boundary layer thickness or a body dimension. More recently, Liepmann and Roshko[11] have pointed out that since these criteria were based on comparison of rarefield flows with solutions applicable to high Reynolds number and incompressible flows, they were inconsistent and could not be expected to be significant.

This problem was further discussed by Lees[12] and Adams and Probstein[9]. Their studies suggest that the continuum, Navier–Stokes equations may be applicable up to the region in which the flow begins to behave like a free molecular flow and that the molecular flow effects might be postponed to much larger values of the free stream Knudsen number than has been often assumed.

The latter is primarily due to an appreciable decrease of the mean free path at the surface of a body in hypervelocity flight. The decrease may result from:

(i) Shock compression upstream of the surface.
(ii) Appreciable cooling of the boundary layer.
(iii) Appreciable pressure gradients at the body surface generated by interaction of the viscous and inviscid regions.

An order of magnitude study[9] indicates the following relations between the Knudsen number based on the ambient mean free path and on the one at the body surface:

(i) $$Kn_\infty \approx r Kn_s$$

where r = ratio of density downstream to upstream of the shock and Kn_s = Knudsen number downstream of a normal shock

(ii) $$Kn_\infty \approx M_\infty^2 Kn_b$$

where Kn_b = Knudsen number in the stagnation region, assuming the surface temperature to be of the order of the ambient temperature.

Since, at hypervelocities r would attain values of the order of 10 to 20, and M_∞ between 10 and 30, the free stream Knudsen numbers would in general be one or more orders of magnitude larger than the ones pertinent to the flow near the body surface.

Thus, if it were assumed that molecular flow effects might become appreciable at local Knudsen numbers of the order of 0·1, then this would correspond to free stream Knudsen numbers of the order of 10 in a cooled stagnation region or one in an uncooled stagnation region.

A similar effect is observed [12] with respect to the Knudsen number based on the boundary layer thickness. When strong viscous interactions are present, the boundary layer thickness varies as $\rho_\infty^{-1/4}$ rather than the usually-assumed $\rho_\infty^{-1/2}$, and the density increases locally as $\rho_\infty^{-1/2}$. Thus, the boundary layer Knudsen number λ/δ is proportional to $\rho_\infty^{-1/4}$ rather than $\rho_\infty^{-1/2}$, i.e. increases much less rapidly with the density decreasing than has been assumed. As a result, the molecular flow effects would be expected to become apparent at much lower ambient densities or Reynolds numbers. This, in fact, has been indicated by experimental measurements of friction on a flat plate[13].

Dynamic Effects. So far, we have considered only the static or equilibrium aspects of real gas effects. However, under conditions of high total enthalpy and low density, the state of a real gas may depend significantly on time. More specifically, it is affected by the time required to attain equilibrium after a quick change of state, such as may be caused by shock compression or rapid expansion. If this so-called relaxation time is of the same order of magnitude as the time taken by an element of the gas to pass through the flow field of a hypervelocity spacecraft, then departures from equilibrium may affect the particular flow field.

We have already stated that, in order to statically simulate real gas effects at high enthalpies, it was probably necessary to duplicate the actual relative velocity and state (enthalpy and entropy). It would now appear that dynamics of real gases would require the exact duplication of physical scale, so that the ratio of relaxation time to flow time was reproduced.

Lacking reliable experimental data on dynamic behavior of air, it would be unrealistic at the present time to indicate limits beyond which the relaxation effects could not be ignored and actual scale would have to be duplicated. However, it would seem that, at high enough velocities and low enough densities, exact duplication of flight conditions rather than simulation might be necessary. The parallel with the gas flows involving combustion is perhaps appropriate, and our inability to satisfactorily scale down the latter phenomena might be significant in relation to simulation of hypervelocity flows of real gases.

In hypervelocity facilities which rely on expansion from a reservoir containing air at the required isentropic stagnation conditions, the dynamics of the expansion process in the nozzle has to be considered. If

the expansion were sufficiently rapid, the air would be expected to "freeze" upstream of the test section and the ambient model conditions would be that of a non-equilibrium gas, of composition and state different from the ones required. Equilibrium could be reached again as a result of compression near the model. This would be the inverse of the situation encountered in actual flight, where ambient air is in equilibrium and relaxation effects appear in the flow field of the vehicle.

It is thus clear that in expansion-type facilities, the problem of equilibrium in ambient flow is of fundamental importance and requires close investigation. Since it is difficult to envisage means by which, under conditions favorable to freezing, it could be evaded, it is necessary, first, to estimate the extent of freezing and, secondly, the effects on model flow field.

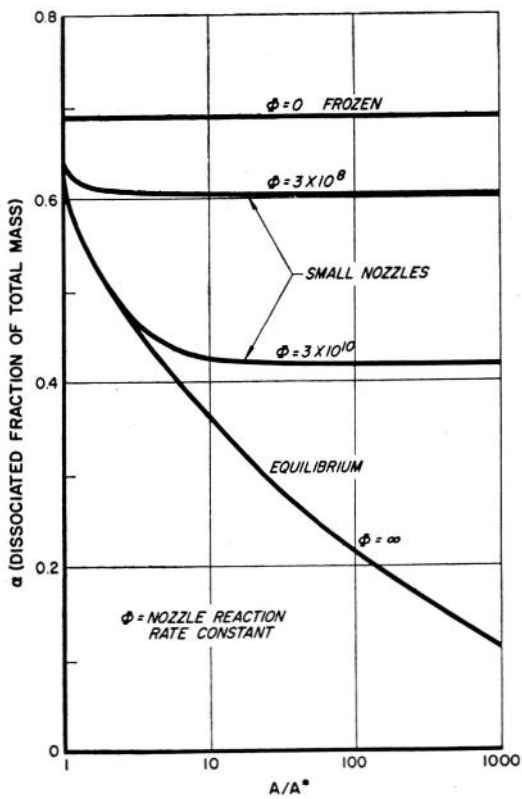

FIG. 3. Freezing of flow in nozzle expansion[14].

Both these aspects have been recently investigated by Bray[14]. His results suggest that if freezing occurs in a nozzle, it will proceed rapidly and the gas will remain frozen and its composition substantially constant downstream of this region, irrespective of further expansion or flow in

a constant area test section. This is indicated in Fig. 3, from Ref. 14. Moreover, it is found that the gas would be partly frozen over a very wide range of values of the reaction rate parameter (a ratio of 10^8), so that, increasing the linear dimensions of the nozzle or reducing the expansion angle would have only a small effect on the frozen flow. It was estimated that a ten-fold increase in linear scale would reduce the non-equilibrium component by less than 10% of the total mass.

It would thus appear likely that, under conditions of sufficiently high stagnation enthalpy and low density, a partly frozen flow would be obtained in the test section. Its effects downstream of a normal shock (formed, e.g. ahead of a blunt-nose body) are found to consist mainly of a larger entropy increase (i.e. reduction of density and pressure) and a correspondingly larger separation of shock from the body. The changes in density and pressure (of the order of 25%) would be expected to affect heat transfer rate and drag. The stand-off distance, which is a function of density ratio across the shock, may increase by a factor as large as 2, since the density ratio is decreased by both a larger density in the frozen flow and a smaller downstream density. Bray suggests that this might be, in effect, a sensitive method to detect frozen flow and to measure the nozzle reaction rate constant.

As already stated, present numerical estimates of relaxation effects in rapid expansions are uncertain pending more accurate determination of the rate constants. The following are tentative estimates only. For example, it is found that for stagnation conditions of 8900°K, 350 atm pressure and 25 atm density*, corresponding to flight at 12,000 ft/sec and 160,000 ft altitude, the non-equilibrium may involve 15% of the stagnation enthalpy in a 10° nozzle terminating in a 1 ft test section.

3. HYPERSONIC WIND TUNNELS

The test Mach number, limited to a value of about 5 by air liquefaction at normal stagnation temperatures, has been extended by conventional hypersonic wind tunnels to Mach numbers below 10. Considerable amount of information has been already published on the design of such hypersonic facilities. Our object here will be to consider recent progress in the critical fields of heater and nozzle development. Some aspects of test techniques will be also briefly discussed.

Heaters

Hypersonic wind tunnels operate usually at stagnation pressures not exceeding 300 atm, it being in practice difficult to contain much higher pressures at the high temperatures required and to adequately cool the nozzle throat region. The corresponding minimum temperature for

* A density of 1 atm is equal to the density at a pressure of 1 atm and a temperature of 273°K (0·0804 lb/ft³ for air).

prevention of air saturation is indicated in Fig. 4. At a Mach number of 10, it amounts to about 1060°K.

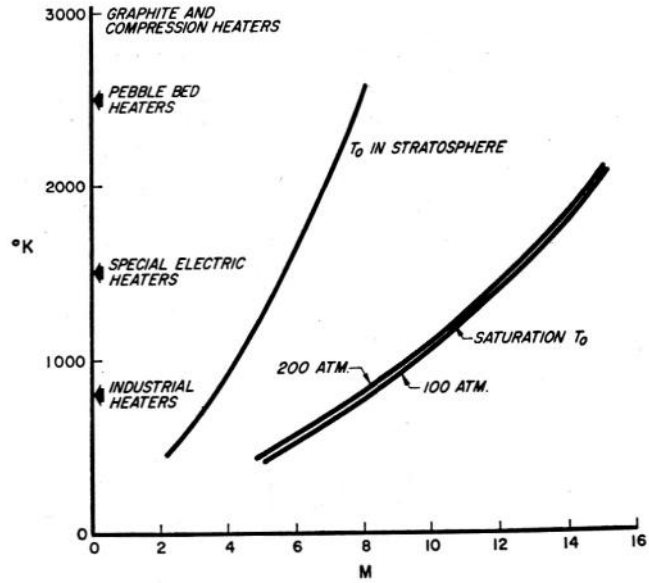

FIG. 4. Flight, air saturation, and heater temperatures.

In the lower temperature range, up to about 800°K, industrial heaters of the electrical-resistance or of the combustion type are available. Higher temperatures can be obtained either with special electrical resistance

TABLE 1

	Thoria (ThO_2)	Stabilized Zirconia (ZrO_2+ 5% CaO)	Magnesia (MgO)	Alumina (Al_2O_3)
Melting point, °K	3240	2550	2800	2200
Max. useful temp. in still air, °K	2700	2500	2400	1900
Density, lb/ft³	625	335	225	250
Sp. heat (CHU/lb°K at 1300°K)	0·07	0·16	0·31	0·28

heaters or with storage-type heaters. For example, temperatures as high as 1450°K have been obtained[15] with a small, 250 V electric heater using Kanthal wire heating elements wound on alumina rods and insulated with Fiberfrax. Results obtained recently with experimental electric

heaters of a different type are discussed later.

The characteristics of some oxide ceramics[16], which can be used as a heat-storage medium, are listed on page 139.

From the point of view of maximum usable temperature, thoria is an attractive material, although precautions would have to be taken in view of its radioactive nature.

The storage medium is usually heated by passing hot combustion products or by means of electrical heating elements. With hydrocarbon fuels, the maximum combustion temperatures reach about 2400°K at atmospheric pressure, and in excess of 3000°K if pure oxygen were used. In a small experimental heater[17] of this type air was heated to about 2500°K. Electrical-resistance heating elements (e.g. silicon carbide) are available for peak temperatures of about 1900°K. Still higher temperatures might

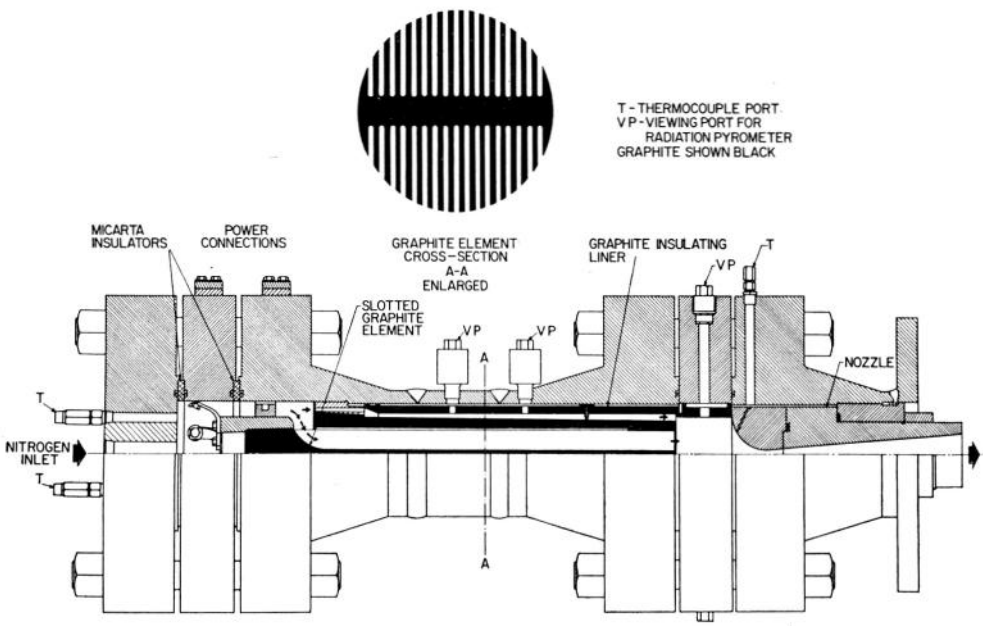

FIG. 5. Construction of an electric heater with graphite resistance elements.

be obtained by rapid compression. A system of this type[18] is expected to compress 100 lb of air to a pressure of 2000 lb/in^2 and a temperature of 2800°K, and to deliver the compressed air at a constant pressure. The compressor is used as a second-stage heater, the initial heating being accomplished in an alumina storage heater.

It is evident from the above rudimentary review of heater types in use with hypersonic wind tunnels, that at the present time:

(i) Heaters for continuous operation at temperatures much in excess of 1000°K are not generally available.

(ii) Heaters available for higher temperatures, such as storage or compression-type heaters, do not lend themselves easily to fast response control of the temperature.

Heater development has been in progress in the Gas Dynamics Facility, A.E.D.C., for some time now with a view of eliminating both of these deficiencies, and particularly since it was desired to develop means of dynamic trajectory simulation.

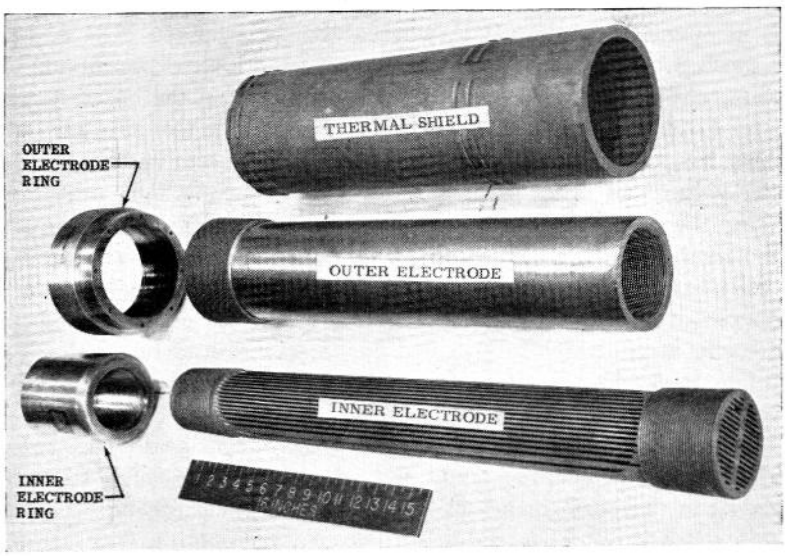

FIG. 6. Graphite heater elements.

In order to achieve the required temperature control characteristics, the direct, forced-convection, electrical-resistance type heater was selected. From the experience with the existing electric heaters of this type, it was realized that many design and fabrication difficulties were due to the simultaneous occurrence of high pressures, temperatures, and voltages. The last was the only factor which could be eliminated and heater elements working at voltages below 100 V were developed. The reduction of operating voltage significantly decreased the insulation difficulties and enabled construction of a compact heater. The construction of this heater, in which a graphite resistance element is used with nitrogen as the working fluid, is shown in Figs. 5 and 6.

In parallel with the development of the graphite-nitrogen heater, electric heaters using slow-oxidizing, metal elements are being developed. In small-scale tests of a heating element passage (D, in Table 2, p. 143),

measuring $0{\cdot}05 \times 1 \times 24$ in. and made of stainless steel (Series 321), a heat dissipation of up to 250,000 B.t.u./ft^2/hr was measured, at an element temperature of 1380°K and with outlet air at 1130°K. In view of favorable experience with the graphite heater, it is intended to use the same type of resistance element construction with stainless steel and Kanthal*, a high-temperature alloy with a melting-point temperature of about 1800°K and a usable continuous-service temperature of 1600°K. Further increases in temperature might be possible with Super-Kanthal ($MoSi_2$) and oxide ceramics.

The performances of some conventional and experimental electric heaters are compared in Table 2. A and B are high-voltage heaters; A is in operation at the GDF, whereas B is a proposed NACA design. C is the O.S.U. Kanthal-Fiberfrax heater. D and E are experimental GDF heaters, and F and G are the designs proposed on the basis of experimental GDF development to date. It is noticeable that the low-voltage heaters have a heat flux per unit element surface area and also per unit heater volume an order of magnitude larger than the high-voltage ones.

From the point of view of attainment of highest temperature, graphite is the most attractive element material, since it melts at about 4000°K at pressures of the order of 100 atm. Its physical strength increases with temperature increasing up to about 2800°K. Moreover, it is inexpensive and easily machinable. In order to enable graphite to be used with air at high temperatures, suitable oxidation-resistant coatings are being developed by the industry.

This survey indicates that there is, at present, considerable scope in the field of heater development and that significant improvements may be expected in the performance of both storage and electric-type heaters.

Hypersonic Nozzles

Two-Dimensional vs. *Axi-symmetric.* The main difficulties encountered in the construction of hypersonic wind tunnel nozzles are essentially due to three factors: very large area expansions, high thermal and pressure stresses which may occur in the nozzle throat region, and adverse viscous effects.

In order to minimize these difficulties, it would be natural to choose a design which would insure dimensional stability of the throat region and a uniform boundary layer. Theoretically, these requirements are best satisfied by an axi-symmetric design, whereas the two-dimensional one is the least suitable. Nevertheless, during the first decade of hypersonic tunnel development, these were not the prevailing views and, in fact, it is only recently that axi-symmetric nozzles found acceptance. It is therefore interesting to examine how, through arguments which were generally accepted as sound, solutions now regarded as unsatisfactory were arrived at.

* Produced by Aktiebolaget Kanthal, Hallstahammar, Sweden.

TABLE 2

Heaters	High voltage		Medium voltage	Graphite	Single Steel element	Slotted element	
	A	B	C	D	E	F	G
Line voltage, V	2300	2300	250	56	24·5	90	90
Element material	Nichrome	Kanthal A–1	Kanthal A–1	Graphite AGX	Stainless 321	Stainless 314	Stainless 446
Max. power, kW	4500	5000	600	2200	25·5	3000	3270
Area for heat transfer, in.^{2}	49,500	58,400	5,000	2620	50·5	2520	9300
Heat flux per unit element surface area kW/in.^{2}	0·09	0·086	0·12	0·84	0·52	1·19	0·35
Heat flux per unit volume† kW/ft^3	49·5	67·5	40·8	2980	—	1120	1220
Volume† of heater, ft^3	91	74	14·7	0·74	—	2·68	2·68
Design max. pressure, psi	3930	5000	4000	4000	2500	4000	4000
Design max. air discharge temp., °K	1070	1530	1550	2480	1090	1090	1090
Heater element geometry	Two concentric round tubes	Round tubes in clusters of 7	0·044 in. dia wire on alumina rods	0·093 in. slotted element, Fig. 6	0·05 by 1 in. flattened tube	0·051 by 0·5 in. rectangular slots	0·075 by 1 in. rectangular slots

† Internal volume of heater pressure shell.
Due to extensive insulation of pressure shell, the "flow volume" of heater C is only 2 ft^3.

Briefly, it was reasoned that two-dimensional nozzles are required to provide Mach number variation, and that, with adjustable but initially highly flat flexible plates, a highly uniform flow could be obtained in the test section. Additional reasons, such as convenient installation of windows in the flat side walls, ease of computation of inviscid nozzle contours and, if flexible plates were used, ease of applying a correction for the boundary layer, were also mentioned.

On the other hand, a somewhat unspecified fear of so-called focusing effects of axi-symmetric nozzles was invariably brought into the picture.

It seems that these arguments can be summed up by stating that "conventional supersonic nozzles should also provide the best solution for generation of hypersonic flow".

Although such a view can be dispelled by even a cursory analysis of the kind here presented, it is nevertheless largely through adverse experience that two-dimensional nozzles are being abandoned for use in hypersonic wind tunnels.

Considering that, at the time, the largest hypersonic wind tunnels were of the order of 1 ft square, and that, as pointed out before, the aerodynamic requirements for Mach number variation in small steps decrease as Mach number increases, the requirement for Mach number variability appears unwarranted. It would seem preferable to exchange complete nozzles, a small number of which would adequately cover the hypersonic Mach number range. Moreover, two-dimensional design in general, and use of flexible plates in particular, pose very serious sealing and throat design problems. In fact, conventional techniques may be inadequate[5] to cool throats of nozzles operating at high Reynolds numbers.

From the point of view of flow uniformity, the two-dimensional design seems to be definitely undesirable, for two reasons: (i) extreme sensitivity of the flow uniformity to throat region configuration, and (ii) highly nonuniform distribution of boundary layer between the flat and the curved nozzle walls.

For example, one-dimensional flow relations indicate that a change of 0·001 in. in the throat gap (0·022 in. wide) of a Mach number 10 nozzle in a 1 ft square tunnel, would cause a 1% change in Mach number and a 7% change in static pressure. That this method in fact predicts correctly the effects of throat distortion has been verified experimentally[19] using a small $M = 5$ nozzle. It is thus clear that it would be extremely difficult, under conditions of high pressure and temperature, to maintain stability of the two-dimensional throat region within the desired limits.

The second factor, concerning boundary-layer flow in two-dimensional nozzles, is perhaps the more fundamental one, in that it may altogether preclude the possibility of obtaining a highly uniform hypersonic flow in a two-dimensional nozzle.

Due to transverse pressure gradients, strong secondary boundary-layer flows develop which tend to reduce the boundary layer thickness on the

curved walls and increase it towards the center of the flat walls. This phenomenon, experimentally observed already in 1950[20, 21], is indicated in Figs. 7, 8, and 9. In Fig. 7 the distribution of turbulent boundary

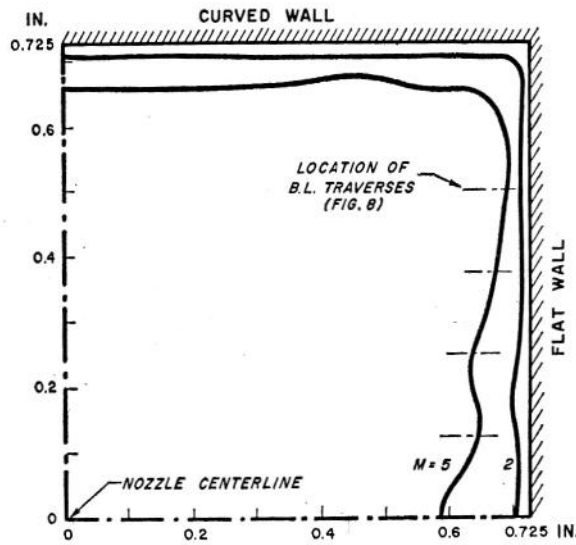

FIG. 7. Distribution of boundary layer displacement thickness at exit of a two-dimensional nozzle at $M = 2$ and 5[21].

layer displacement thickness at the exit of $M = 2$ and 5 two-dimensional nozzles (length to exit height ratio 2·36 and 3·64 respectively, max. wall deflection = 0·6 of Prandtl–Meyer angle) is shown. While at $M = 2$ the boundary layer thickness is approximately equal on curve and flat walls, at $M = 5$ appreciable thickening occurs near the center of flat walls. Corresponding profiles of boundary layer on flat wall, at $M = 5$, are shown in Fig. 8, at various distances from the centerline. On the centerline, the profile has a characteristic "step" shape with an inflection point. Similar boundary layer profiles, shown in Fig. 9, were observed at $M = 6{\cdot}86$ in an 11 in. hypersonic tunnel[20].

Since, for mechanical reasons, the flat walls are usually parallel*, it is customary to apply the boundary layer correction for both flat and curved walls to the curved walls alone. Although such procedure produces a more nearly uniform flow on the longitudinal centerline, the off-axis flow cannot be uniform. The boundary layer growth on the flat walls causes the flow to converge in planes normal to the flat walls and parallel to the centerline. Inasmuch as the contoured walls are over-corrected for their own boundary layer, the flow in the planes parallel to the flat walls diverges.

* In some designs slightly divergent flat walls were used to reduce adverse effects here discussed.

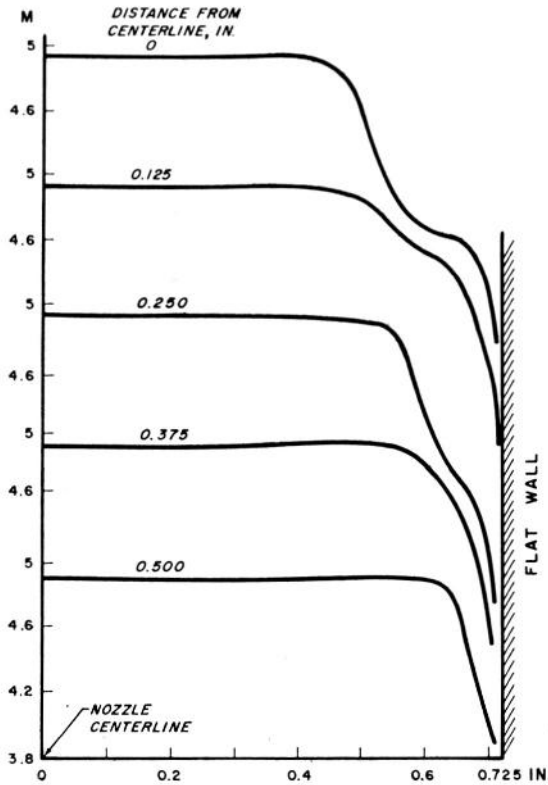

FIG. 8. Boundary layer profiles on flat wall of $M = 5$ nozzle at various distances from centerline (see Fig. 7)[21].

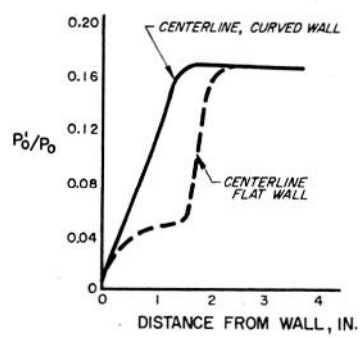

FIG. 9. Pitot pressure distribution in the boundary layer on flat and curved walls in the test region of a $M = 6{\cdot}86$ nozzle[20].

Since the boundary layer thickness increases with Mach number, these effects are accentuated at high Mach numbers.

The other supposed advantages of two-dimensional nozzles are also highly questionable. For example, it is doubtful whether sufficient control can be exerted over the deflection of flexible plates to take full advantage of their initial flatness, and it is not certain whether such extreme precision is actually required.

At high Mach numbers, the variation of static pressure on the centerline of a symmetrical nozzle is given by $\Delta p/p = -2\gamma M \Delta\alpha$. We then find that, theoretically, a 1% variation in static pressure at a Mach number of 5 corresponds to a change in the slope of the walls of about 0·04°, whereas at a Mach number of 10 corresponds to only 0·02° Experience indicates that in conventional, cold supersonic nozzles, it is difficult to control the plate curvature to less than 0·05°, so that even with flexible plates, one would not expect to achieve the precision theoretically required at hypersonic Mach numbers. Moreover, in view of very thick boundary layers present in hypersonic nozzles downstream of the throat, these theoretical requirements may be in practice excessive. Future development of axi-symmetric, hypersonic nozzles will undoubtedly throw some light on this problem.

There appears to be no reason to insist on windows mounted flush with the walls since, at high Mach numbers, disturbances caused at the test section station would not reach the model. As regards computational difficulties, these, although severe when compared with the classical Busemann method, are certainly not insurmountable.

The significance of focusing effects in internal, axi-symmetrical flow

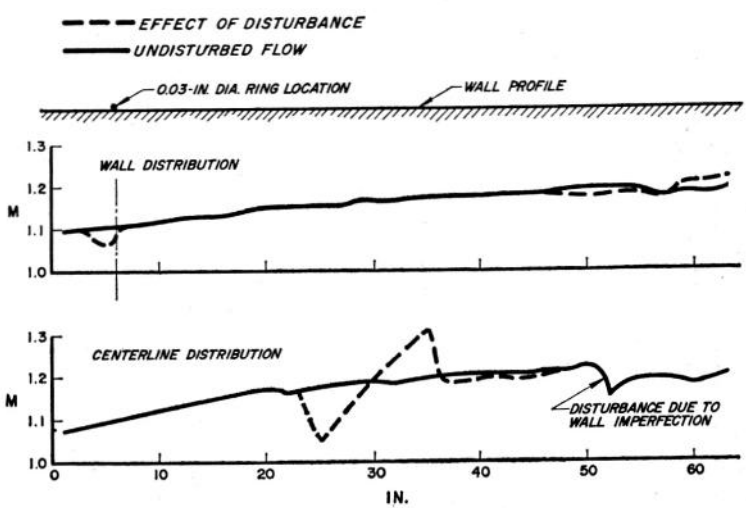

FIG. 10. Focusing of disturbance in an 8 ft dia. $M = 1{\cdot}2$ axi-symmetric Nozzle[22].

is more difficult to assess, particularly in view of the dearth of experimental data. However, as early as 1950, it was demonstrated[22] that a satisfactory axi-symmetric nozzle for a Mach number of 1·2 could be designed and built, and that boundary layer growth could be accurately estimated, to the extent that position of the aerodynamic throat was predicted to within 1 in. in a 96 in. dia. nozzle. In the same series of tests, the focusing properties of the nozzle were investigated by placing an axi-symmetric 0·03 in. dia. disturbance on the nozzle wall. The results, in terms of Mach number distribution on the wall and on the nozzle centerline, are shown in Fig. 10. Appreciable focusing occurred, the disturbance being amplified to $\pm 0{\cdot}13\,M$ on the axis and reduced to about $\pm 0{\cdot}025\,M$ on intersecting the wall downstream. The ratio of the boundary layer displacement thickness at the location of the wire to the wire diameter was about 8·7. These tests have shown that by precise control of the nozzle contour, a flow uniform to within $\pm 0{\cdot}02\,M$ could be obtained, and that random, localized disturbances did not affect the flow significantly.

Although the focusing property of axi-symmetric nozzles could undoubtedly lead to serious difficulties, it is expected that the reduction of these effects to acceptable limits is a matter of development of both design and fabrication techniques, just as much as the perfection of supersonic, two-dimensional nozzles had been.

Development of Axi-symmetric Nozzles. Historically, the first axi-symmetric nozzles for higher supersonic Mach numbers have been probably developed for low-density wind tunnels, as part of a programme of low-density research initiated in 1947 at the University of California[23]. This was done mainly to reduce the boundary layer effects at the very low Reynolds numbers of tests. Axi-symmetric nozzles were used with hot air (up to 900°K, $M = 3{\cdot}8$) in the Bofors supersonic blowdown tunnel in Sweden in 1954[24]. Around 1956, they were used in hypersonic tunnels at the Polytechnic Institute of Brooklyn[18] and the Ohio State University[15]. It was Ferri *et al.* who first presented, in a paper[18] published in 1955, a cogent argument for the use of hypersonic, axi-symmetric nozzles in preference to the two-dimensional ones. This interesting original discussion is reproduced in the Appendix to this paper.

Following the success achieved at the P.I.B. and O.S.U. with axi-symmetric nozzles, and as a result of growing realization of difficulties encountered with two-dimensional ones, most of the hypersonic wind tunnels in the United States for Mach numbers greater than 7 or 8 are being designed, since about 1957, with axi-symmetric nozzles, and progress is being made in the techniques of computation of profiles and boundary layers, cooling and manufacture. We shall here attempt to highlight some of the more significant developments in this rapidly-moving field.

Computation of Profiles. With the use of large electronic computers, the actual computation of an inviscid, axi-symmetric nozzle profile is completed in a matter of minutes. A family of over 40 profiles, ranging from

$M = 6$ to $M = 20$, for expansion angles from 6 to 12° and for values of γ from 1·2 to 1·67 will be included in a forthcoming AGARDograph[25].

Computation of Boundary Layer Growth. Progress has been made in methods of calculation of the turbulent boundary layer growth in axi-symmetric nozzles. In Fig. 11, experimental measurements of the displace-

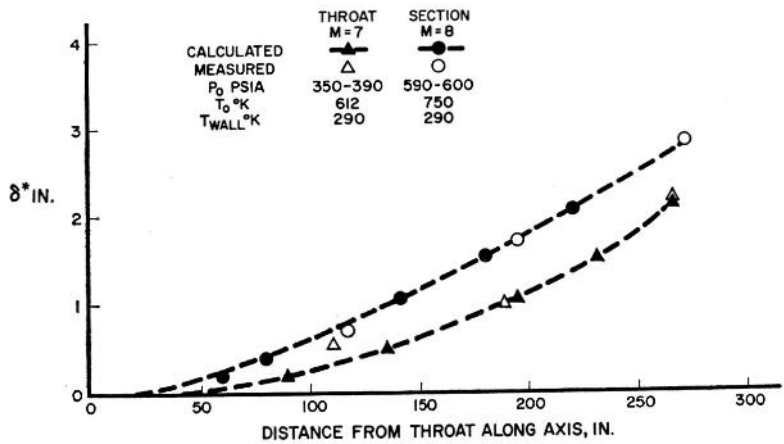

FIG. 11. Experimental and theoretical boundary layer growth in a 10°, 50 in. dia. conical nozzle.

ment thickness δ^* in a 50 in. dia. conical nozzle are compared with theoretical predictions made using a method developed by J. C. Sivells of the Gas Dynamics Facility, A.E.D.C. The method is based on Stewartson's transformation of von Kármán's momentum equation.

Cooling of the Throat Region. From the point of view of dimensional stability and amount of heat transferred to the walls, an axi-symmetric nozzle possesses the optimum shape. The ratio of perimeters of a two-dimensional to a circular throat for nozzles having equal exit dimensions (i.e. side of the square equal to diameter), is given by

$$\frac{2(x + 1/x)}{\pi} \approx \frac{2x}{\pi}$$

at large Mach numbers, with $x = A/A^*$. This ratio attains the values of 8·8 at $M = 8$ and 14·75 at $M = 10$. At moderate temperatures, of the order of 900°K, simple throat cooling by water-jacketing is adequate. Small nozzles (3 in. dia.) in which boundary layer remains laminar, have been successfully operated[15] at temperatures of 1500°K and stagnation pressures of 250 atm, with a water-cooled, copper-throat section. Larger nozzles (12 in. dia.), made of mild steel and nickel-plated, water-cooled only in the throat region, were run[26] at 40 atm pressure and 900°K stagnation temperature for periods of up to 20 sec.

An ingenious design of the nozzle throat, for operation under conditions of high heat flux, has been developed by Ferri[18]. The nozzle throat is

surrounded by a cooling passage so shaped that when cool air at the tunnel stagnation pressure is admitted, pressures across the throat wall are equalized. Thus, separation of pressure and temperature stresses is achieved, and thin throat walls can be used. They are cooled by vaporization of water sprayed into the cooling passage. If a larger than necessary amount of water is introduced, the wall temperature remains substantially constant for a wide range of heat transfer rates, only the amount of vaporized water changing and the process being thus self-stabilizing.

Other methods, such as e.g. helium or air film cooling, are being developed to extend the pressure-temperature range of hypersonic wind tunnels.

Manufacture of Axi-symmetric Nozzles. Basically, axi-symmetric nozzles can be made by either of the two methods: direct machining, e.g. on a contour lathe, or reproduction, e.g. by precision casting or electroforming.

For manufacture of smaller nozzles, up to about 1 ft dia., the latter method has been successfully used in the United States*. It consists of, first, construction of a mandrel on a precision contour lathe and, secondly, of electroforming of the nozzle walls. The mandrel is made of a material which can be easily machined and polished, is stiff and can acquire a chemically-inert surface. A free-machining stainless steel has been found suitable for this purpose. If it is desired to preserve the mandrel, it can be

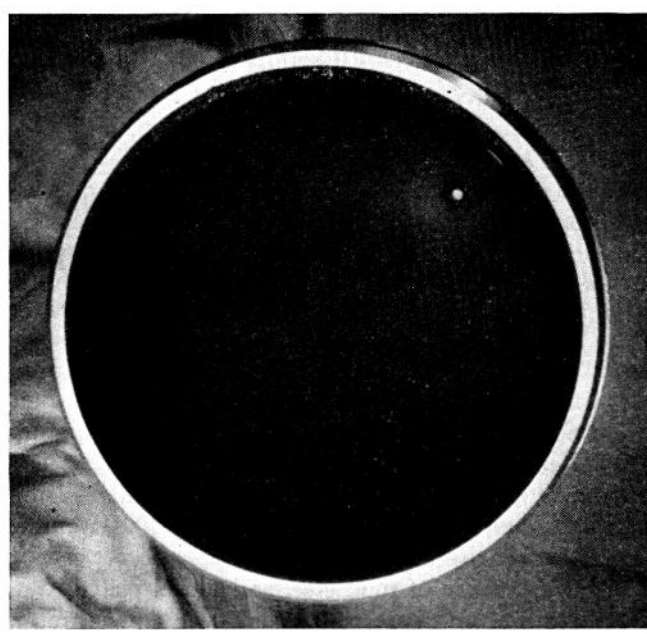

FIG. 12a. $M = 8{\cdot}8$ electroformed hypersonic nozzle.

* This method is described in detail in Ref. 27.

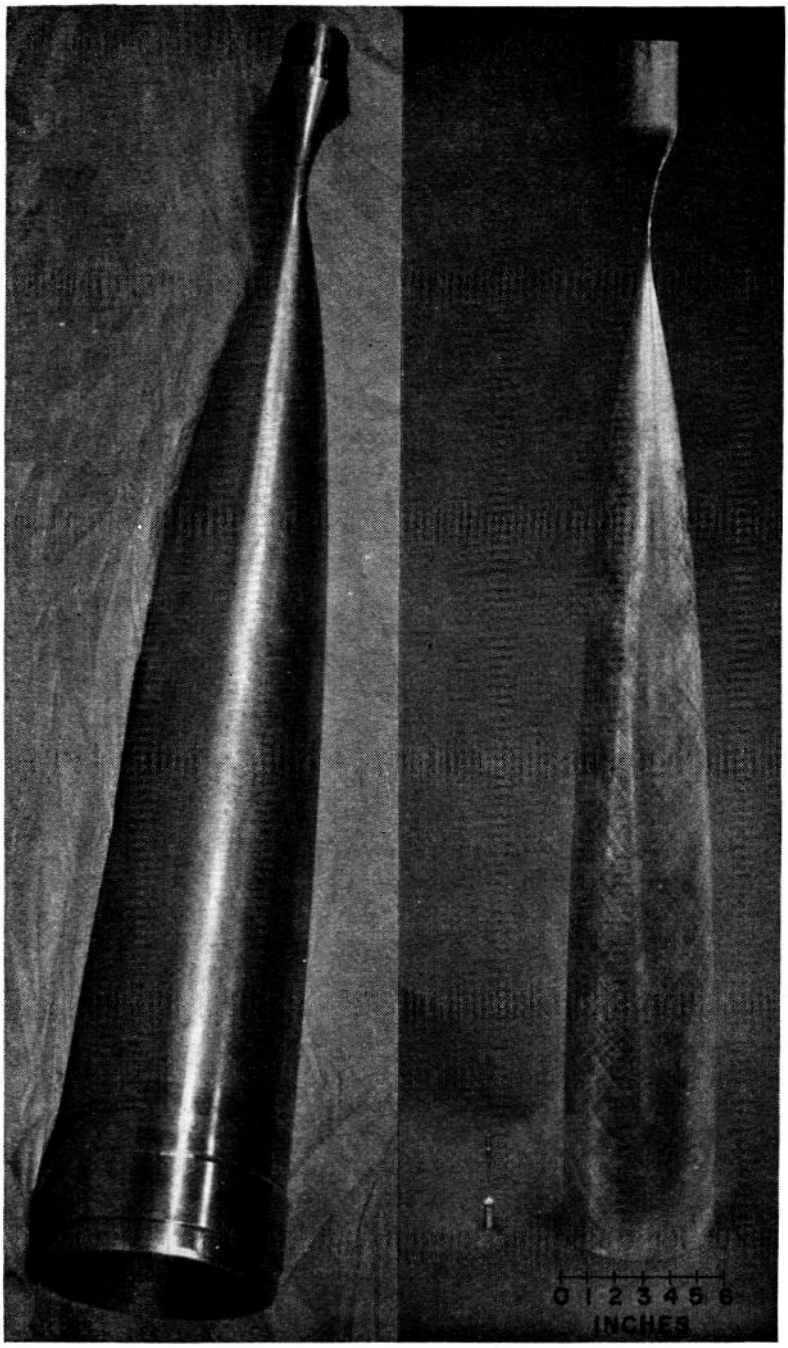

FIG. 12b. $M = 8{\cdot}8$ electroformed hypersonic nozzle and nozzle mandrel.

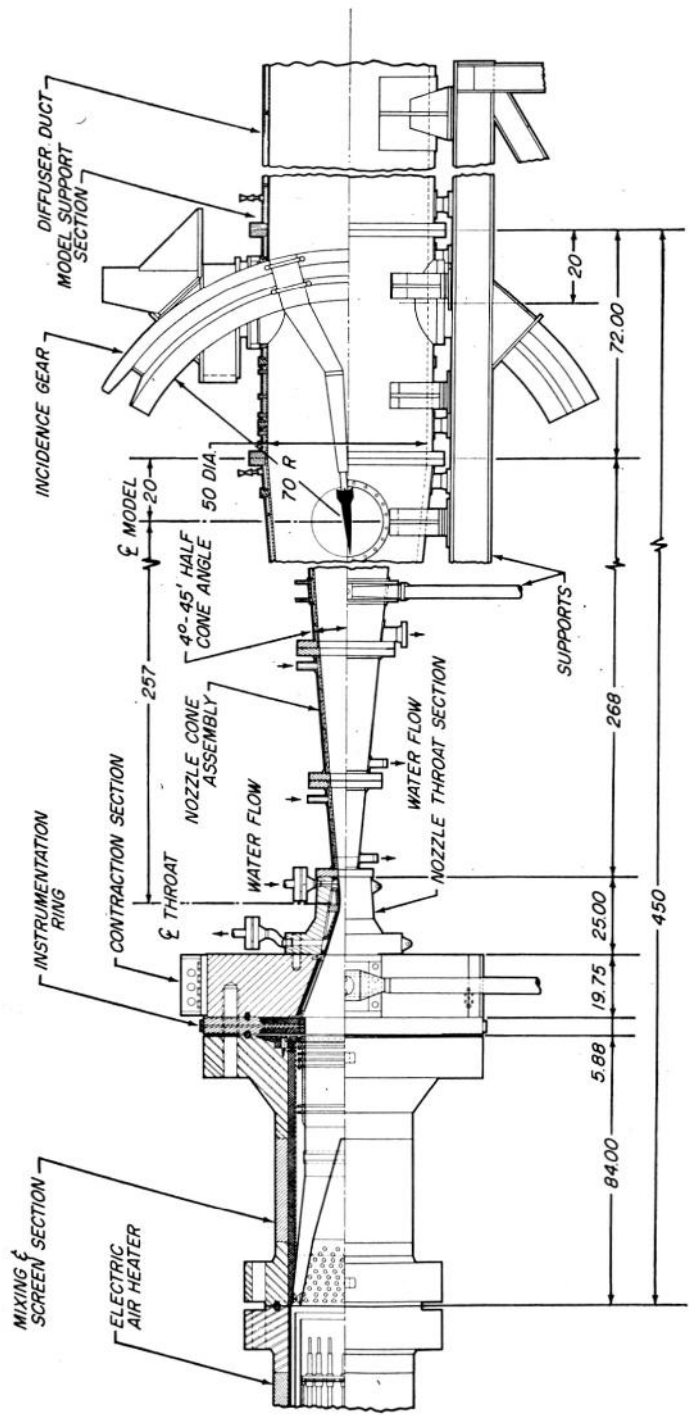

FIG. 13. GDF 50 in. dia. hypersonic wind tunnel.

built in two sections, joined at the throat. For electrodeposition on the mandrel, nickel was found to be a suitable and inexpensive material. Special methods were developed for withdrawal of the mandrel. Examples of a mandrel and an electroformed, 5 in. dia. nozzle, for a Mach number of 8·8 are shown in Fig. 12.

For larger hypersonic tunnels, axi-symmetric nozzles are usually built up of several fabricated or cast, and precision-machined sections.

An Example of Hypersonic Tunnel Design. We have already pointed out that the construction of hypersonic wind tunnels has badly lagged in relation to development of hypervelocity vehicles. In an attempt to temporarily fill the gap, a very simple, but yet effective, hypersonic wind tunnel has been recently put into operation at the GDF. Its construction is shown in Fig. 13, with the details of the nozzle throat section given in

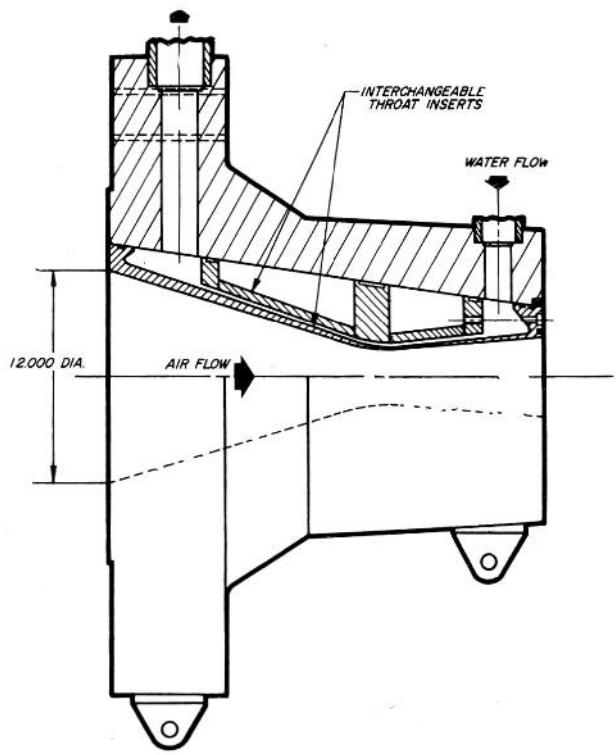

FIG. 14. Throat assembly for a 50 in. dia. hypersonic nozzle.

Fig. 14. The tunnel has a 50 in. dia. test section and a conical, water-cooled nozzle assembled from four sections. It has been operating at $M = 7$, $T_0 = 600°$ K and $P_0 = 30$ atm. A Mach number gradient of 1·7%/ft exists in the test section and closely corresponds to the one calculated for a source flow, provided the boundary layer is taken into account. Mach number 8 can be obtained by inserting a different throat

liner in the throat section. The interim conical nozzles are being replaced by contoured ones.

Hypersonic Tunnel Test Techniques. The techniques of force and pressure measurements in hypersonic tunnels essentially do not differ from the ones used at supersonic speeds. Internal model, water- or air-cooled balances and pressure-measuring systems with transducers and scanning valves located as near to the pressure hole as possible are standard practice.

On the other hand, heat-transfer investigations under conditions of cooled boundary layers require the use of relatively cold models and taking of transient temperature readings. The model must therefore be shielded immediately prior to temperature measurements. This can be accomplished by retracting the model into the wind tunnel wall, where it can be cooled, and "injecting" it into the airstream for the purpose of test, or by direct cooling by means of a water spray from upstream. Another method is to shield the model by means of retractable covers or "cooling shoes". This system, as used in the GDF 50 in. tunnel, is shown in Fig. 15. Cooling air is ducted to the shoes through the cooling-shoe supports mounted in the test section ports, with model positioned at zero incidence. After the required degree of cooling has been achieved, the cooling shoes are retracted by hydraulic actuators into position shown in Fig. 15, and the model is pitched to the preselected angle of attack.

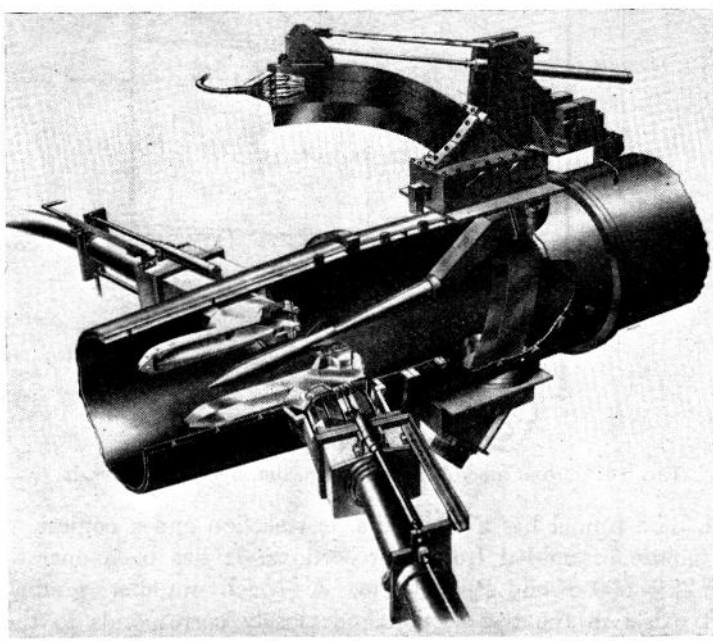

FIG. 15. Cooling shoe and model support system, GDF 50 in. dia. hypersonic wind tunnel.

The outputs of 100 thermocouples are then digitally recorded every 0·25 sec. After completion of test, the model is returned to zero incidence for cooling in preparation of the next run. Incidentally, the cooling shoes provide protection to the model on starting and stopping of the tunnel.

A number of different instrumentation techniques are used to obtain heat-transfer rates to models. With models having thin skins, the heat conduction in a direction parallel to the model surface can be neglected and local heat transfer determined from the rate of change of skin temperature and its heat capacity. Alternatively, plugs insulated from the model skin can be used[26] and heat transfer calculated from readings of temperature of the exposed end, on the assumption of semi-infinite slab, initially at uniform temperature.

It may be noted that for force and heat-transfer tests an intermittent tunnel is probably preferable to a continuous one, the latter being more suitable for pressure plotting tests.

Range of Operation

In Fig. 4 are plotted the minimum stagnation temperatures required to obtain condensation-free flow at stagnation pressures of 100 to 200 atm, and also the actual stagnation temperatures in flight in the stratosphere. On the same graph are indicated the approximate upper limits of various types of electric heaters, as previously discussed.

It is immediately evident from this figure that duplication of flight enthalpy is not likely to be achieved in hypersonic wind tunnels beyond a Mach number of about 8, due to the heater limitation alone. On the other hand, from the temperature point of view, Mach number simulation would be possible up to Mach numbers of the order of 16.

The range of simulation obtainable with hypersonic wind tunnels with respect to Mach and Reynolds numbers is shown in Fig. 1 in the altitude-velocity plane. The curves have been drawn for 200 atm stagnation pressure and for corresponding saturation stagnation temperature (Fig. 4). Also, since at altitudes between 30,000 ft and 120,000 ft the velocity of sound equals approximately 1000 ft/sec, the velocity scale has been treated as the Mach number scale for these curves.

The lower curve corresponds to Re/ft equal in the tunnel and in flight. For the upper one, the Reynolds number for a one-tenth-scale model is equal to that of the full model in flight.

It is seen that large hypersonic wind tunnels may well cover the lower velocity region of lifting trajectories.

4. SHOCK TUBES

Shock tubes are probably the first test facilities which could simulate air enthalpies similar to those encountered in hypervelocity flight. Although the principle of operation of shock tubes was discovered by P. Vieille in 1899, at about the time at which first wind tunnels were

built, it was only in the last decade that shock tubes were developed into useful experimental tools. The literature on the shock-tube techniques is very extensive and we shall therefore limit the discussion to the range and limitations of the applications, as indicated by results obtained in the United States.

Domain of Simulation

In a classical, constant-section shock tube, a diaphragm separates high-pressure "driver" gas from the low-pressure "driven" gas. Following bursting of the diaphragm, a normal shock propagates into the low-pressure portion of the tube, compresses and sets in motion the "driven" gas. If the tube is closed at the downstream end, the shock reflects, further compresses and brings to rest the "driven" gas.

These two phases of flow of the driven gas are of interest in relation to hypervelocity flight. They are also being used in studies[28] of physical and chemical properties of air and other gases at high enthalpies. Rate constants of reactions, emissivity and electrical conductivity of gases at high temperatures are being measured. Also, interactions between magnetic fields and the flow of electrically-conducting fluids are studied and foundations of magnetogasdynamics developed. The ability of shock tubes to produce high enthalpy gases of high purity is a significant factor in this work.

However, we shall not be here concerned with the basic physico-chemical studies but rather with the more direct application of shock tubes to investigation of hypervelocity flight.

When a model is placed in the low-pressure section of a shock tube, it experiences, first, a brief unsteady flow period as the normal shock passes, and later an essentially steady flow, until the arrival of the driver gas or of the disturbances originating at the tube ends. However, the maximum Mach number attainable in air behind an advancing shock does not exceed about 3, for infinitely strong shocks.* We have thus in a shock tube an unusual situation of flow of a very high enthalpy and a relatively low Mach number and we therefore should examine to what extent it can serve to simulate the high Mach number, hypervelocity flight conditions.

We may remark immediately that in general for flows about the same model and with equal total enthalpies but at different Mach numbers, the shock system about the model will be different and therefore the entropy distribution in the model flow field will not be duplicated. Because the flow is non-isentropic, even the duplication of the pressure distribution on the model will not make the inviscid flow fields similar.

Nevertheless, there is a type of flow of great interest to hypervelocity flight which can be well simulated in a shock tube, namely the flow in the stagnation region of a blunt body[28, 29, 30]. Since in this case the rate

* For a perfect gas with $\gamma = 1{\cdot}4$ the limit is 1·89.

of heat transfer is of prime importance, it is the boundary layer flow which requires simulation. This will be achieved provided the inviscid flow immediately outside the boundary layer is duplicated. The latter, in fact, is well predicted by the Newtonian approximation, which does not depend on Mach number.

We thus conclude that, provided any two parameters such as enthalpy and pressure are duplicated at a blunt stagnation point, the flow near the latter and, hence, the heat transfer rate are well simulated. However, the heat transfer rate is proportional to the square root of the velocity gradient along the edge of the boundary layer, or, using Newtonian approximation, inversely proportional to the square root of the nose radius. Thus a model scale effect is introduced, but simulation of Mach number is not required.

The above considerations are obviously valid for equilibrium conditions throughout the flow and for completely "frozen" flows. However, the boundary layer flows which are chemically dynamic depend on the ratio of the diffusion time to the lifetime of the species or the recombination rate parameter which is proportional to the linear scale and to the square of the density. Therefore an additional scale effect is introduced. If the effects of density on "real gas" properties at a given enthalpy were neglected, then small-scale, non-equilibrium flows would correspond to full-scale conditions at much higher density altitudes.

From the point of view of heat transfer rate at the stagnation point, the chemical dynamics of the boundary layer flow is fortunately not too important, if the Lewis number if near unity and the wall catalises atomic recombination. For air, with $Le = 1{\cdot}4$, the difference was estimated[30] to amount to 5% between a frozen and an equilibrium flow.

Still another problem connected with the stagnation region heat transfer rate is that of the radiation from the high enthalpy air. Since radiated energy is proportional to the thickness of the radiating gas layer, it would be difficult to detect in small-scale experiments and yet, if it represented an appreciable fraction of the full-scale convective heat flux, the determination of its magnitude would be essential.

On the basis of recent shock tube measurements of emissivity of air at high temperatures, it has been estimated[28] that, in equilibrium conditions, the radiative heat transfer is a small fraction (0·1) of the convective heat transfer at the stagnation point, at $M = 20$ and 120,000 ft altitude. This would indicate that under conditions of large convective heat transfer rate, the effects of gas radiation are indeed small. Their relative significance would increase with altitude increasing and possibly under non equilibrium conditions.

The region in which shock tubes have been successfully applied to stagnation point heat-transfer measurements is indicated in the velocity-altitude plane in Fig. 1. It covers very adequately the significant entry phase of ballistic trajectories, including satellite entry velocity. As discussed in the next section, attempts are being made to extend the application of shock

tubes to conventional aerodynamic tests of models at high Mach numbers.

Limitations of Shock Tube Technique

The application of shock tubes to model tests is primarily limited by the short run times available and small working section sizes. The latter are a consequence, for structural reasons, of the large pressures required to develop high enthalpy flows and of the difficulties of constructing and bursting under such conditions large diaphragms. Because of strong attenuation of flow by the viscous effects, excessive length to diameter ratios cannot be used and since the run time is proportional to shock tube length, only short runs are possible with small-diameter tubes.

The actual run times vary from about 1 to $\frac{1}{10}$ msec, the attenuation of the initial shock velocity not exceeding 10%, and increasing to 20% in the extreme cases of high density and turbulent boundary layer flow on the tube walls[29]. The determination of ambient flow conditions depends on the measurement of shock velocity and the state of the "driven" gas at rest, and on the assumption of equilibrium. The ambient conditions are then computed with the aid of, for example, a Mollier diagram.

Because of extremely short run times, the model measurements in shock tubes have been limited, until recently, to heat transfer rate and optical observation of flow. Suitable heat-transfer gauges, of thin resistance thermometer, and of calorimetric type, with a microsecond response time, have been developed[29].

In view of the severe Mach number limitations of shock tubes, attempts are being made[31, 32] to develop hypersonic shock tube tunnels, by expanding in a divergent nozzle the high enthalpy flow following the shock. For moderate Mach numbers (≈ 6) a single divergent nozzle is attached to the tube end, whereas for higher ones (≈ 10), a convergent-divergent nozzle is used, the shock reflecting from the nozzle throat as from a closed tube end. With this scheme of operation, an appreciably higher "driver" pressure has to be used to obtain a given flow density in the test section, since the entropy of the "driven" gas is additionally increased in compression by the reflected shock. At a shock Mach number of 10 in air, the driver and driven gas pressures have to be increased by a factor of about 2·5 relative to the non-reflective operation.

The main difficulties encountered with the development of shock tube tunnels are due to flow attenuation and short running time. The latter can be increased by the reflected shock method and by suitably matching the state of the "driver" gas at the contact surface so that the reflected shock will pass into the "driver" gas without reflecting any disturbances[31].

So far, running times of the order of 1 to 5 msec have been obtained in shock tube tunnels and mainly heat-transfer measurements were made. Methods of force measurements have not, as yet, been developed.

Since, until recently, it has not been possible to measure pressure in the test section, the determination of Mach number and, hence, of the

other flow variables in shock tube tunnels depended on optical observation of shock wave angles. This is an inherently inaccurate method and, furthermore, depends on the equilibrium assumption. In fact, this is the very same method used to investigate the recombination rates in shock tube experiments.

The shock tube would seem to be most useful in its original form and has already provided valuable data on heat transfer in the stagnation region of blunt-nose models. Other techniques, described below, are capable of providing, at large Mach numbers and enthalpies, and using relatively large models, aerodynamic data of the type obtainable from conventional wind tunnels.

5. FREE PISTON SHOCK TUNNELS*

A facility somewhat similar to the above-mentioned shock tube tunnel of the reflected shock type, has been initiated at the NACA Ames Laboratory[33] and further developed at ARDE (Fort Halstead)[34] and at the University of Southampton. In the free piston shock tunnel the driver and driven gases are separated by a piston, which replaces the contact region of the shock tube tunnel. Following rupture of the diaphragm which initially separates high-pressure driver gas from the piston and the working medium, the piston is accelerated and eventually reaches steady velocity, which is that of the contact surface in a shock tube. At the downstream end of the tube a hypersonic nozzle and another diaphragm are located. Following several reflections of the shock wave from the nozzle entry and the piston, the piston motion eventually damps out, the nozzle diaphragm is ruptured and hypersonic flow established in the nozzle.

It has been estimated[34] that running times, contingent on throat erosion, of the order of hundreds of milliseconds could be obtained with a free-piston shock tunnel.

The potential advantages of the free-piston shock tunnels, compared with the shock-tube tunnels, are the freedom from mixing losses in the contact region and from disturbances which limit the running time.

6. ELECTRIC-ARC-DRIVEN TUNNELS

The electric-arc-driven, so-called "hotshot" wind tunnels are perhaps the most recent newcomers in the field of hypervelocity test facilities. They were developed in the Gas Dynamics Facility, AEDC, during the past three years and during the past year, were used for numerous industrial tests. The history, details of development and operation of hotshot tunnels, and some test results obtained are given in a recently-published paper by R. W. Perry and W. N. MacDermott[35]. Our purpose here shall be to discuss some of the unique characteristics of the hotshot tunnels and their performance.

* Also known as "light gas gun tunnels".

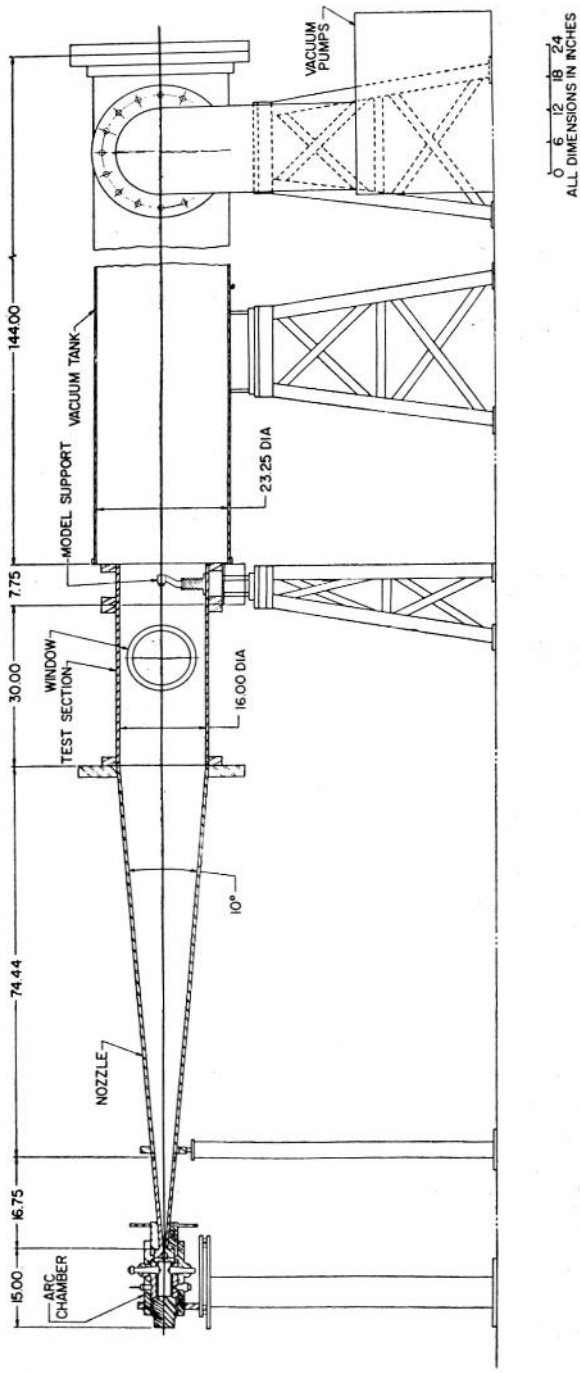

FIG. 16. 16 in. dia. hotshot tunnel.

Design and Instrumentation

In Fig. 16 is shown the first hotshot tunnel, with a 16 in. dia. test section. It consists of an arc-chamber separated by a diaphragm from a 10° conical nozzle, attached to a cylindrical test section and cylindrical vacuum tank. Initially, the arc-chamber is filled with air at moderate pressure (up to 130 atm) and at normal temperature, while the rest of the tunnel is evacuated to a low pressure (about 0·01 mm Hg). The operation of the tunnel consists of discharging stored electrical energy in an arc inside the arc-chamber. This causes a rapid rise in temperature and pressure of the air in the arc-chamber and disintegration of the diaphragm. Following the initial, unsteady phase of flow, a quasi-steady flow is established in the nozzle and test section, the reservoir conditions decaying at a rate dependent on the volume of the arc-chamber in relation to nozzle throat area and on the heat losses to the arc-chamber walls. In practice, 20 to 50 msec of quasi-steady flow are obtained, in which time model measurements can be made.

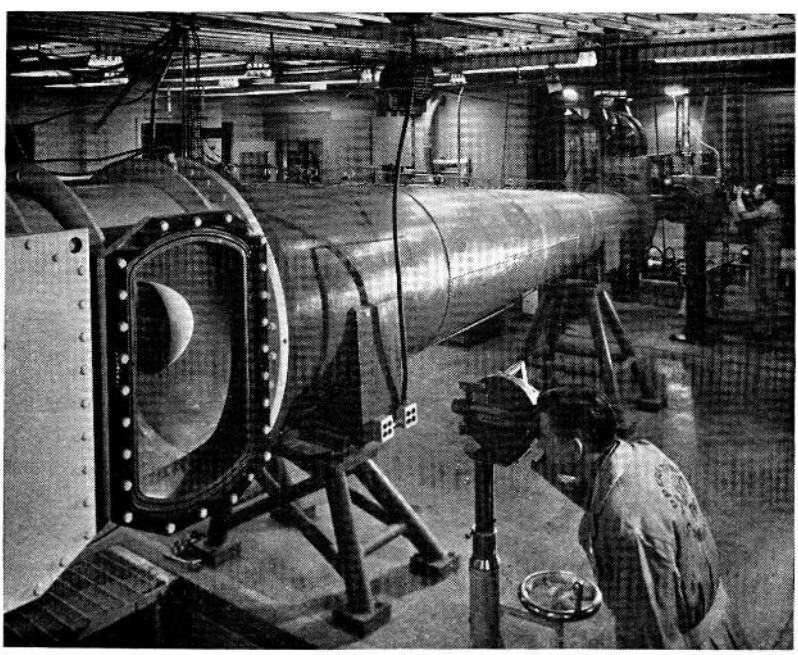

FIG. 17. 50 in. dia. hotshot tunnel.

A similar, but larger, 50 in. dia. hotshot tunnel shown in Fig. 17, is being at present developed, and it is planned to construct eventually a still larger facility which would be capable of near full-scale tests.

The power supply for hotshot tunnels consists of energy storage in capacitors or in magnetic field of a large coil. The latter type of storage,

although at present less efficient, appears to be more economical for energy levels above about 10^6 joules. The 16 in. dia. hotshot tunnel employs capacitor-type storage rated at 10^6 joules (1000 capacitors of 125 μF each at 4000 V), whereas the 50 in. dia. one uses inductive storage rated at 10^7

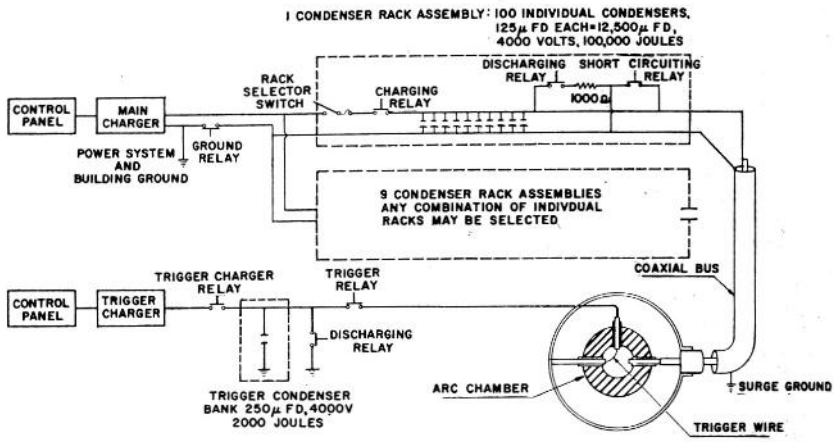

FIG. 18. One million joules capacitor power supply.

joules. The two types of storage are shown schematically in Figs. 18 and 19. With the inductive storage, large currents necessary to store the energy in the field are obtained from a homopolar generator driven by a flywheel.

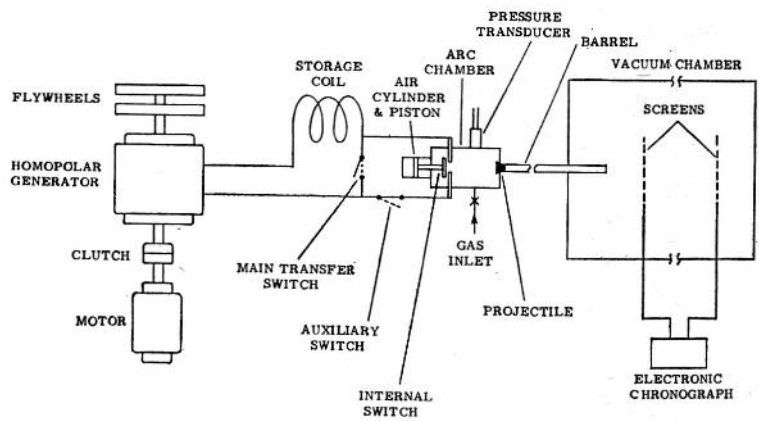

FIG. 19. Ten million joules inductive power supply and electric-arc gun installation.

This brief description of construction and operation of the hotshot-type tunnel indicates close resemblance to a conventional, intermittent wind tunnel. Because of the relatively long running times, it has been possible to use fundamentally similar instrumentation techniques, and to measure, in addition to heat transfer rates, pressures and forces on the models.

It was found that because of the longer running times, thin-film resistance thermometer gauges could not be used, at least in the stagnation region of models and a miniaturized variable-reluctance heat-transfer gauge, of the calorimeter type, was developed (Fig. 20). The heat-sensing element of this gauge consists of a 0·01 in. thick, 0·1875 in. dia. copper ring, contoured to the surface of the model.

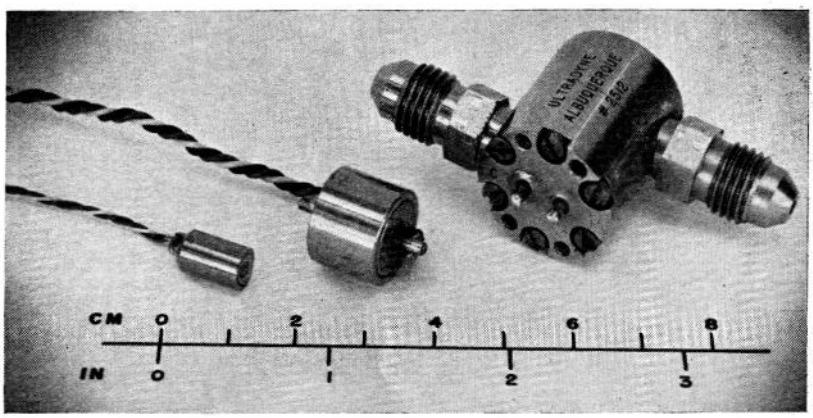

FIG. 20. Heat transfer and pressure transducers for hotshot tunnels.
Left: Miniaturized heat transfer transducer.
Middle: Miniaturized pressure transducer.
Right: Commercial pressure transducer.

Similarly, a special, miniaturized, variable-reluctance pressure transducer was developed (Fig. 20), interchangeable with the heat-transfer gauges. The pressure range covered by this transducer extends from 0·1 mm Hg to 5 lb/in^2.

Forces are measured with strain-gauge balances of conventional design, except for unusually high stiffness and provision of adequate damping. To achieve the required frequency response of 1 to 2 kc, stiff supports and plastic models of small mass are used.

Typical examples of model instrumentation and of results obtained are shown in Figs. 21 to 25.

Arc-chamber and Nozzle Throat

These are the most critical components in the development of hotshot tunnels.

The arc-chamber design difficulties are due to simultaneous requirements of containing air at extreme pressures and temperatures and providing adequate support and insulation for electrodes and transducers. A recently-evolved design of a 4000 atm arc-chamber for use with the inductive power supply, with which shots reaching over 3400 atm pressure were made, is shown in Fig. 26. It consists essentially of a cylindrical pressure

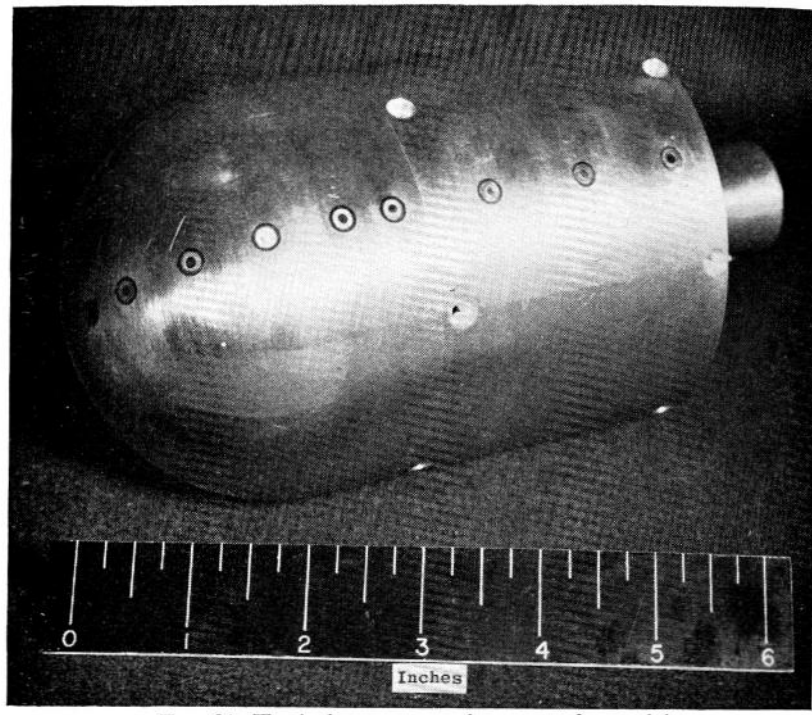

FIG. 21. Typical pressure or heat transfer model.

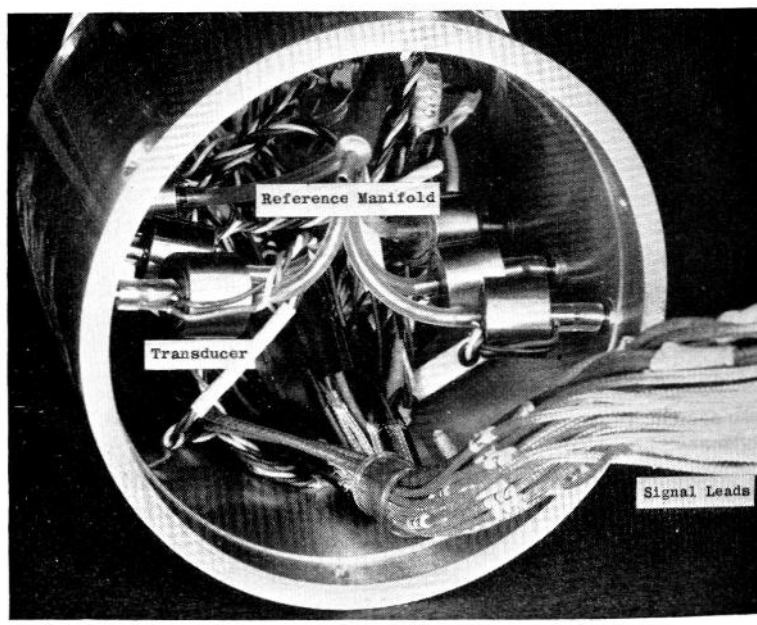

FIG. 22. Typical installation of miniaturized pressure transducers.

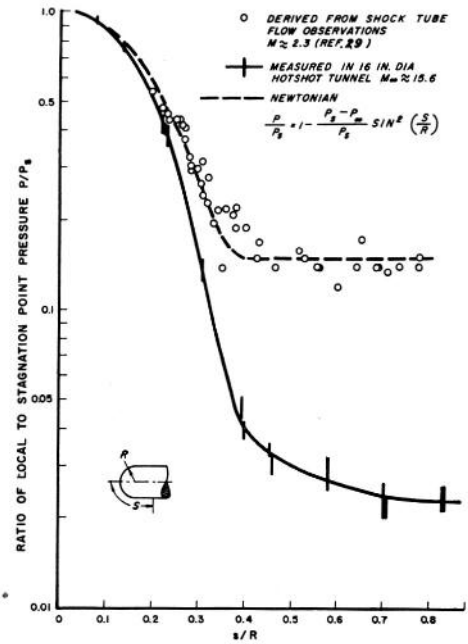

FIG. 23. Pressure distribution on hemisphere cylinder[36].

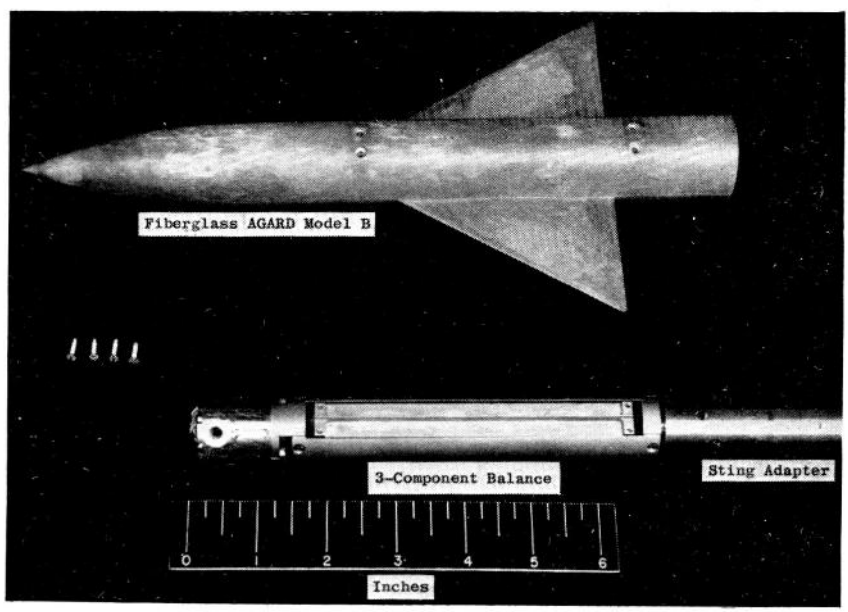

FIG. 24. Three-component balance and AGARD model B.

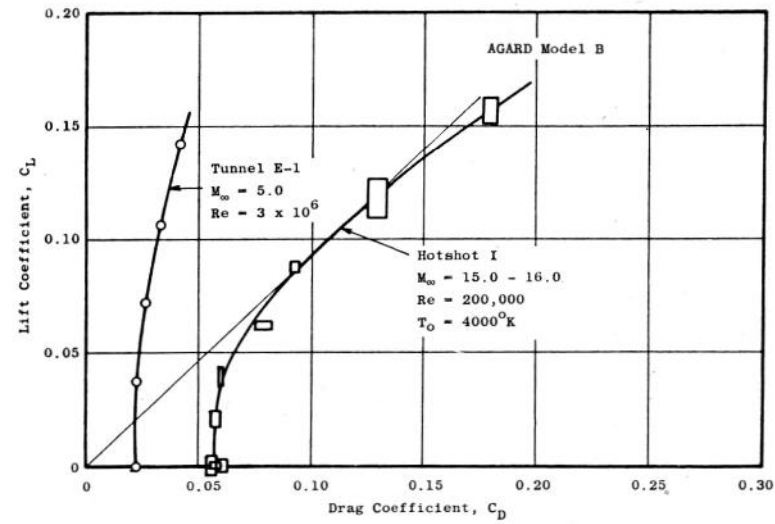

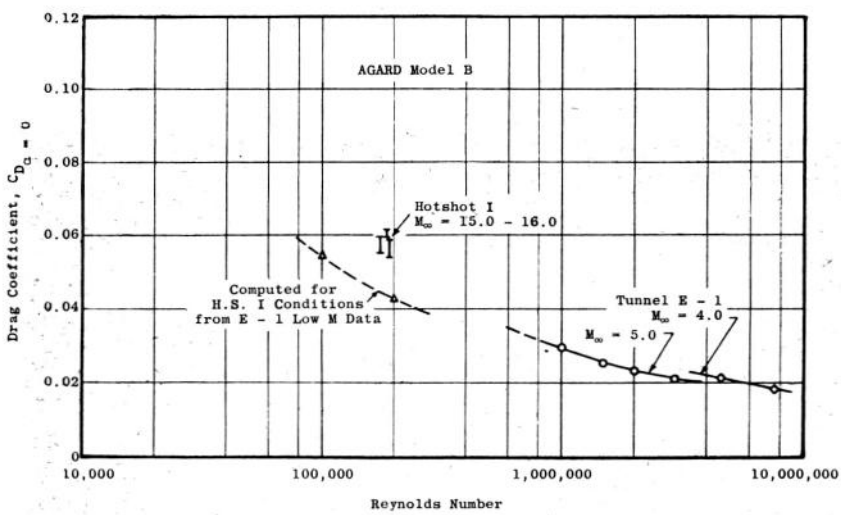

FIG. 25. Lift and drag of AGARD model B at Mach numbers of 5 and 15.

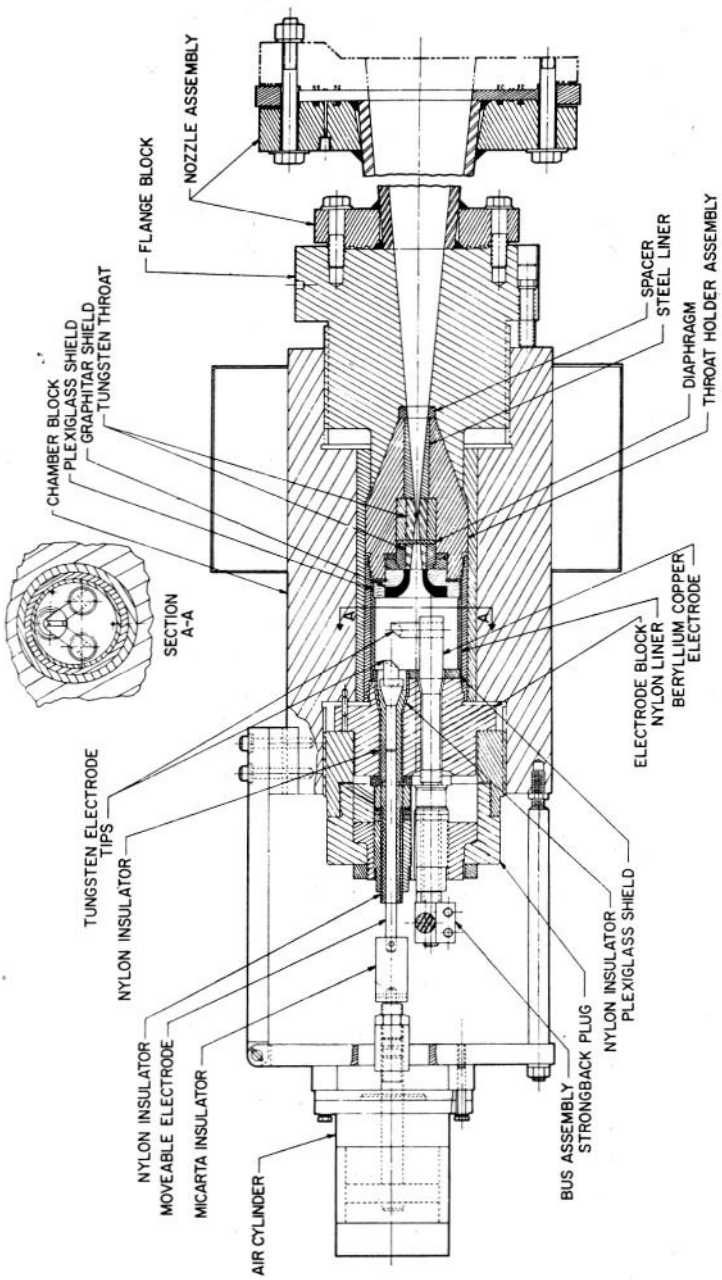

FIG. 26. 4000 atm, 45 in^3 arc chamber.

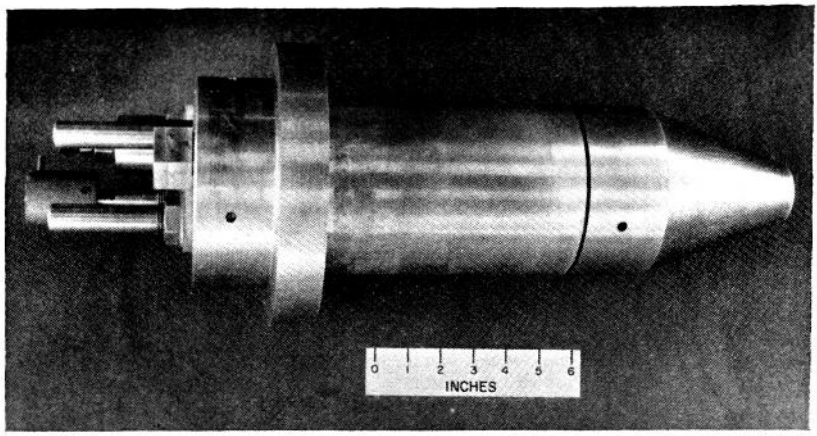

FIG. 27. Removable cartridge containing arc-chamber operating components.

vessel in which a cartridge assembly, shown in Fig. 27, is inserted from the back. The cartridge contains electrodes, transducers, arc-chamber insulating liner, a metal or plastic diaphragm and throat insert. The pressure loads on the electrodes are taken by outside supports so that the insulators are not subjected to them. Moreover, with this type of construction, the whole cartridge assembly is easily replaced should the electrodes or throat become excessively damaged.

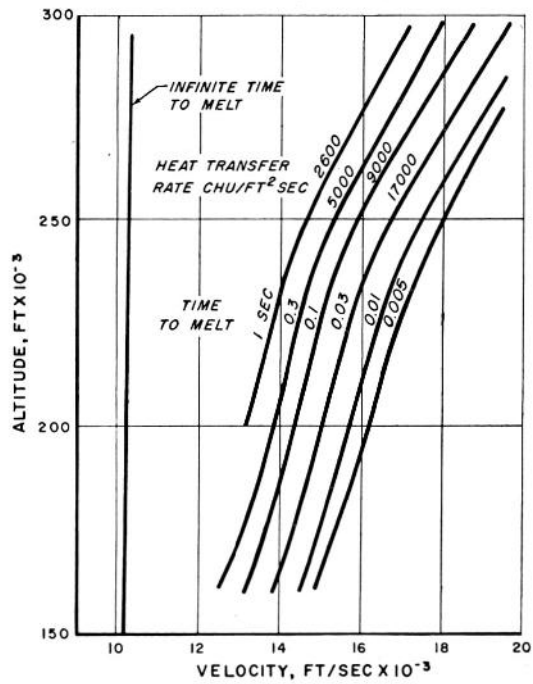

FIG. 28. Time to melt a tungsten throat for flight-simulating tunnel.

In order to reduce throat erosion to minimum, the throat insert is made of tungsten. From a simple analysis of heat transfer to the throat, the times required for the surface to begin to melt, the subsequent rates of erosion and heat transfer rates have been estimated[35] and are shown in terms of altitude-velocity test-section conditions in Fig. 28. It is interesting to note that, at altitudes between 150,000 and 300,000 ft, runs of 10 msec duration appear possible before throat erosion commences, at speeds from 14,000 to 20,000 ft/sec.

It follows that most of the throat erosion probably occurs after the useful portion of the run has been completed. In order to eliminate this damage to the throat, efforts are being made to develop an automatic blow-off valve.

In addition to the fundamental heat transfer aspect, the throat construction presents problems for very small ($<0{\cdot}05$ in. dia.) and for large ($>0{\cdot}2$ in. dia.) throats. In the former case, the difficulties are those of machining tungsten; in the latter, it is difficult to provide a large diaphragm which would withstand initial air pressure. Instead, it may be possible to provide a check valve closing off the throat and automatically opening it after the electrical discharge has taken place.

Power Supply and Switching Problems

As indicated in Fig. 18, with the capacitor-type power supply a trigger discharge is used to initiate the main heating-arc. The efficiency of this type of drive (ratio of energy delivered to the air to the stored energy) was found[37] to depend on the density of air, and increased from about 60 to 70% at a density of 35 atm to about 75 to 95% at a density of 70 atm. The large scatter of the data presumably reflects variable energy losses in the external arcing to ground and in the buss-work due to inductive loads.

The inductive energy storage presents a difficult switching problem in that an interruption of a large current is necessary to cause the arc. Ideally, one would desire to pass the current during "charging" of the coil through the electrodes in the arc-chamber and then open the circuit by moving an electrode connector. In practice, with the arc-chamber sizes so far developed, it was difficult to provide electrodes large enough to accommodate the currents and thus avoid incurring excessive losses and heating, which, incidentally, is detrimental to insulation.

Therefore, a switching system with which coil current is transferred to the arc-chamber just before arcing, has been used as indicated in Fig. 19. During charging, the main transfer switch and the electrode internal switch are closed, while the auxiliary switch is open. To obtain arcing, the auxiliary switch is closed, the main one opened, and finally the electrode switch is pulled. In this process, large losses occur in arcing across the main transfer switch and the overall energy transfer efficiency amounts to only 40 to 60%.

It is hoped that, particularly with larger arc-chambers, it will be possible to develop an electrode design which would permit complete internal switching.

In view of very large d.c. currents carried to the arc-chamber, copper coaxial buses have been used with both types of power supply.

Determination of Test Section Conditions

In hotshot tunnels, which are driven from a constant volume air supply, the flow in the test section is quasi-steady and therefore the variation of free stream parameters with time must be determined for reduction of the model test data. The procedure adopted is based on (i) the knowledge of the initial mass and state of air in the arc-chamber, before mass flow starts, as defined by the initial volume, temperature and pressure, and (ii) the knowledge of the state of the air in the arc-chamber during the run, as determined from the measured pressure and from the density computed from a step-by-step integration of the outflow from the arc-chamber. This procedure requires accurate estimate of the effective cross-sectional area of the throat, which is obtained from a cold air flow throat calibration.

It should be noted that this calculation, while not dependent on an estimate of heat lost to the arc-chamber walls, allows these losses to be evaluated.

The third step in the determination of test section conditions consists of a time record of test section pitot or static pressure. Since the isentropic stagnation conditions are known from (i) and (ii) above, the velocity and state of the air in the test section may be determined from suitable normal shock tables and a Mollier diagram.

The foregoing procedure is based on a number of assumptions, namely thermodynamic equilibrium during expansion, non-contamination of air, constant throat size, and accurate knowledge of air properties at extreme pressures and temperatures.

As already discussed, the first assumption would not be satisfied under conditions of sufficiently low density and high enthalpy, and represents one of the basic problems of hypervelocity tunnel facilities.

The air contamination results from the erosion of tungsten tips of the electrodes and pyrolysis of the arc-chamber lining. The former was found to amount to not more than 4% of the mass of air in a small ($20\ \text{in}^3$) arc-chamber, and its main effect is probably a mild sandblasting of models. The latter might be more significant since it produces gaseous contaminants and consumes oxygen. However, these effects would tend to diminish with the arc-chamber size increasing.

Performance of Hotshot Tunnels

There are a number of factors which determine the range of test section conditions attainable with hotshot tunnels. Perhaps the most rigid limits

are imposed by the maximum pressure to which the arc-chamber can be subjected and the power available.

From the point of view of simulation, it might be desirable to duplicate completely in the test section the atmospheric conditions of flight, that is, the density, temperature, and velocity. The generalized performance of hotshot tunnels for this type of testing is shown in Fig. 29 in

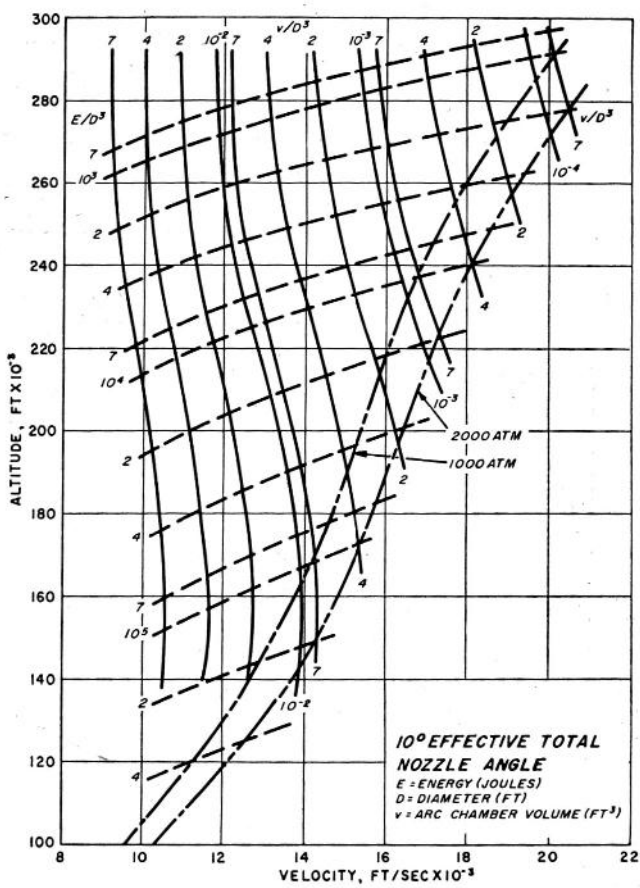

FIG. 29. Generalized performance of hotshot tunnels for flight duplication.

the altitude-velocity plane, in terms of E/D^3 and v/D^3 where E = actual energy supplied to air (joules), v = arc-chamber volume (ft^3) and D = effective test section diameter (ft). In making such performance calculations some assumptions must be made as to the required degree of steadiness of flow in the test section. Here it has been assumed that the outflow through the nozzle in one particular transit time between the arc-chamber and the test section must not exceed 1% of the initial total mass of air in the arc-chamber. The transit times were calculated for constant velocities equal to test section velocities and for conical

nozzles with 10° effective total expansion angle and infinitely small throat. Since the transit time, as defined above, increases in proportion to linear scale, both the arc-chamber volume and the energy requirements vary in proportion to the cube of the linear scale. Thus the absolute steadiness of flow, as measured at one point, increases with tunnel size, but remains constant when, for example, related to changes of parameters over a model length, which varies in proportion to tunnel size.

A different performance chart could be obtained for a constant absolute value of flow decay. For example, a rate of flow equal to 1% of the initial air mass in the arc-chamber per 1 msec could be assumed. The ratio of arc-chamber volumes and energies required on this basis to the ones obtained for particle transit time are shown in Fig. 30 for various effective test section diameters. It will be noticed that for larger tunnels (>2 ft dia.) the particle transit time criterion is the more conservative one at high velocities (>12,000 ft/sec).

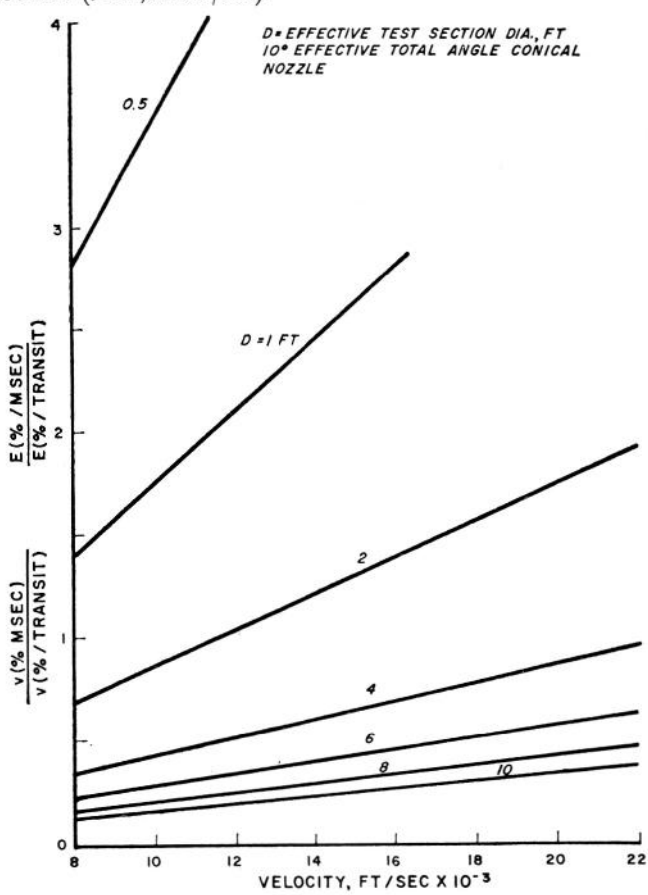

FIG. 30. Ratios of arc chamber volumes (v) and energies (E) based on decay in 1 msec to volumes and energies based on decay in particle transit time.

In considering the decay of reservoir conditions, we have not allowed for heat loss. However, experience with a small 25 in^3 arc-chamber has shown[37] that heat losses are in the range from 10^3 to 10^4 B.t.u./ft^2 sec, and thus correspond to about 1% enthalpy decrease per msec. This effect is therefore not too serious, and would diminish adversely with the scale of the tunnel.

The generalized performance chart (Fig. 29) indicates that, for a given test section size, the available energy determines essentially the minimum altitude for flight duplication, whereas the arc-chamber volume limits the minimum velocity. Since, in a given installation, the maximum energy available may be the least flexible factor, it is clear that low altitudes might be covered with small test sections.

In Fig. 29 also the structural arc-chamber limits are indicated for peak pressures of 1000 and 2000 atm. They impose a severe limitation for attainment of high velocities at lower altitudes.

Depending on the design and manufacture of diaphragm and throat, further limits might be imposed by the minimum and maximum permissible throat sizes. These limits would be a function of the actual throat

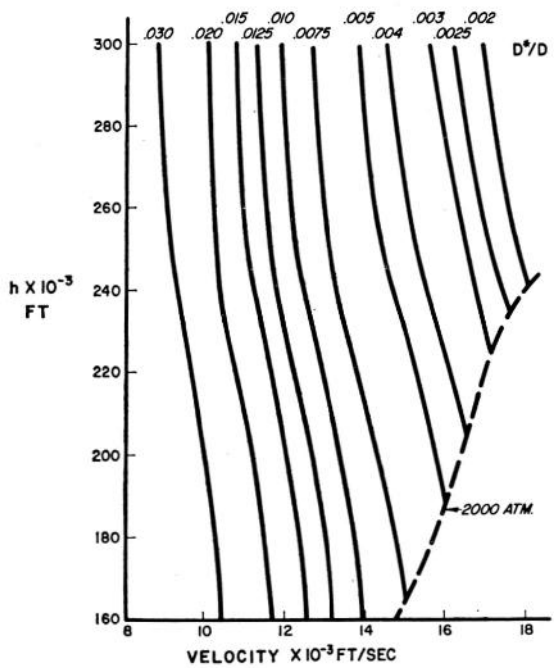

FIG. 31. Effective nozzle throat to exit diameter ratios for flight duplication.

size and can be determined from Fig. 31, in which ratio D^*/D of throat to effective test section diameter as required for flight duplication is given in terms of velocity and altitude.

Based on Fig. 29, the flight duplication envelope of a 50 in. effective diameter hotshot tunnel, using an effective 5×10^7 joules power supply and a 4000 in^3, 2000 or 4000 atm arc-chamber, is shown in Fig. 32 and

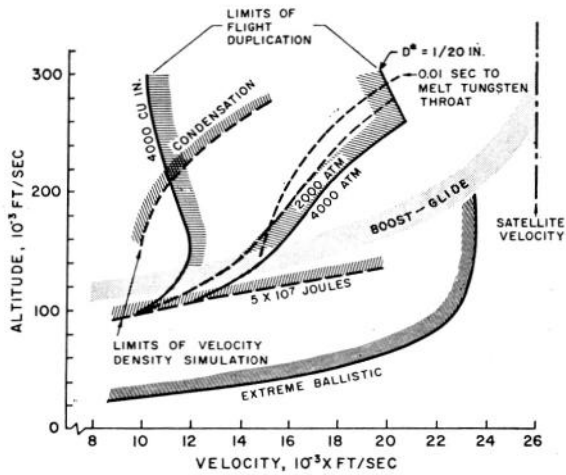

FIG. 32. Regions of flight duplication and velocity-density simulation with a 50 in. dia. hotshot tunnel.

Fig. 1. It is seen that with the chosen limits, 100,000 ft is the minimum altitude of duplication. Also, the 2000 atm pressure limit is closely followed by the 10 msec run time before a tungsten throat begins to melt.

In preparing the generalized performance chart for flight duplication

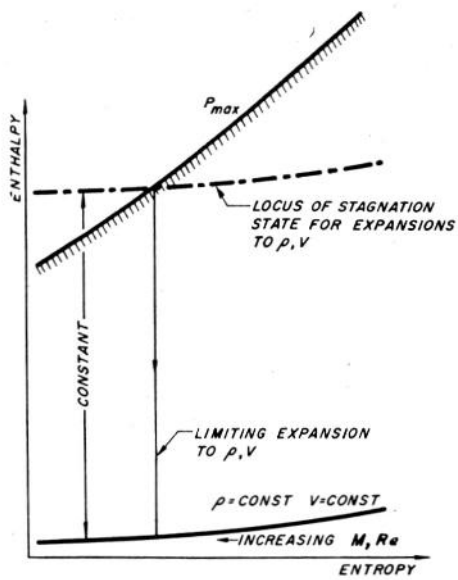

FIG. 33. Expansions from a maximum stagnation pressure.

we have considered a family of isentropic expansions which always had, as an end-point, the atmospheric ambient conditions. However, a much wider range of velocities can be covered if exact duplication is not achieved. For example, assuming that, irrespective of test section size, the maximum arc-chamber pressure is limited to a constant, P_{max} value, we may theoretically consider all expansions starting from pressures equal to or smaller than P_{max}. In practice other factors, such as available energy, throat erosion and test section size would further limit the actual range of operation. However, some general conclusions can be reached as to the expansions requiring minimum energy and attaining maximum Mach and Reynolds numbers, for a given velocity and density in the test section.

Consider a Mollier diagram (Fig. 33), in which the locus of stagnation conditions for expansions to constant velocity V and density ρ is drawn, together with the limiting pressure P_{max}. It is evident that to attain ρ, V, the minimum stagnation enthalpy corresponds to the highest possible pressure P_{max}. Since this expansion also results in the lowest end temperature, the highest Mach and Reynolds numbers are simultaneously reached. Smaller Mach and Reynolds numbers can be obtained in expansions from smaller pressures and higher enthalpies.

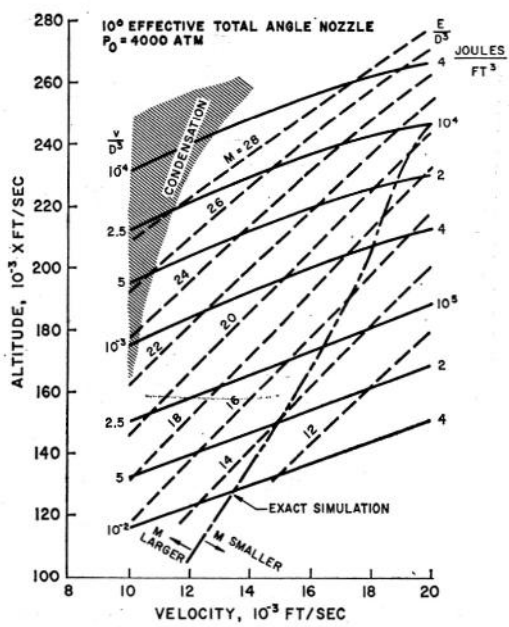

FIG. 34. Generalized performance of hotshot tunnels for velocity-density simulation, $P_{max} = 4000$ atm.

Based on the above considerations, a generalized performance chart for velocity-density simulation has been drawn in Fig. 34, for a constant $P_{max} = 4000$ atm and for the decay based on the particle transit time

(as for Fig. 29). Since for a constant pressure, the ratio of energy to volume is approximately constant*, therefore, only one set of curves is shown for both v/D^3 and E/D^3†. The Mach numbers and the locus of flight duplication are also indicated.

The velocity-density type of simulation is subject to another limit, namely air liquefaction, at lower velocities and high Mach numbers. The condensation region is shown shaded in Fig. 34.

The area of velocity-density simulation for a 50 in. effective diameter hotshot tunnel, with an effective 5×10^7 joules power supply and a 4000 in^3, 4000 atm arc-chamber, is shown in Figs. 1 and 32. Compared with the flight duplication performance, a much wider region of velocities, at altitudes above 100,000 ft, is covered.

The envelopes for flight duplication and for velocity-density simulation indicate that hotshot tunnels are particularly well suited to investigation of boost-glide trajectories.

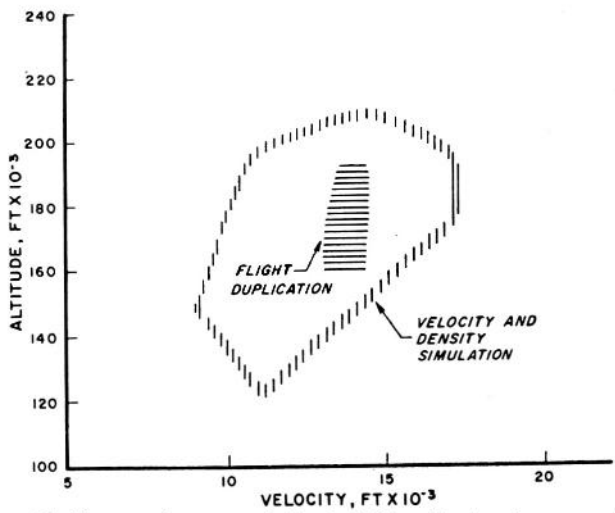

FIG. 35. Range of tests made in the 16 in. dia. hotshot tunnel.

In Fig. 35 the range of conditions actually covered in model tests in a 16 in. dia. hotshot tunnel is indicated. Two areas are shown, corresponding to exact flight duplication and to velocity and density simulation only.

Plasma Jets

In recent years another type of facility, generally known as plasma jet, capable of producing high enthalpy flow and using electric arc drive, has been developed. As the term indicates, the working fluid does not resemble air; the original, German water-stabilized arc produces a mixture of

* At 4000 atm, $E/v \approx 4 \times 10^7$ joules/ft^3 $\approx 1{\cdot}4 \times 10^6$ joules/l.

† Within the accuracy of Figs. 29 and 34, the energy curves are identical.

dissociated and ionized oxygen and hydrogen, contaminated with electrode materials. More recently, arc-powered air jets are being developed[38] and efforts are being made to increase their size and density. For continuous operation, the power requirements are large and the problem of throat erosion becomes increasingly difficult with density increasing. In fact, the hotshot tunnels here described may be regarded as the upper limit, insofar as size and density is concerned, of the present development of arc-powered jets.

7. LOW-DENSITY TEST FACILITIES

In recent years, considerable progress has been made in attaining lower densities and larger mean free paths in the so-called "low density" wind tunnels. In particular, the two-phase cycle, introduced by Chuan[39], offers a practical means of reaching very low pressures, down to 10^{-13} atm. With this cycle, the working gas, after passing through the test section, is cooled to its saturation temperature, condensed and then transferred to a higher pressure, at which the condensate is evaporated and the resulting gas brought back to the stagnation conditions. For the lowest densities, a helium refrigerator is used.

The presently-operating[40] low-density wind tunnels reach velocities of about 2500 ft/sec and Mach numbers of up to about 6 (Fig. 1), and facilities are planned to extend this range to $M \approx 10$. The corresponding velocities do not exceed 5000 ft/sec and there is a fundamental difficulty in reaching much larger ones while maintaining the desired composition of the working gas.

The problem is that of maintaining equilibrium throughout expansion of air from conditions of high enthalpy and low density. If it were not for that, low density, hypervelocity tunnels could be operated using, for example, the hotshot electric-arc drive technique. Evidently, this problem would not arise in hypervelocity range tests.

It is also pertinent to mention a second difficulty of low-density facilities. When the mean free path is large in relation to a model dimension, it is, for reasonably-sized models, also large in relation to test section diameter. For example, Devienne *et al.*[41] have obtained a Mach number 4 flow in a 1·6 in. dia. nozzle with a m.f.p. equal to the nozzle radius. The question of tunnel interference then arises, since the boundary conditions do not correspond to the case of an unbounded fluid. As pointed out by Liepmann and Roshko[11] even in this latter, ideal case, it is difficult to define the proper boundary conditions at infinity.

8. HYPERVELOCITY RANGES

In the past, the ballistic range technique has been severely limited by the type of information which it could supply and, to a lesser extent, by the model velocities attainable. We shall indicate here some of the recent advances made in these two fields.

Telemetering from Models

The conventional range technique essentially consists of determination of model attitude and trajectory in space and time, by means of observations made at a discreet number of stations. From this data, certain steady and unsteady aerodynamic characteristics of a model can be calculated. In addition, from optical observations of flow about a model, information can be obtained on boundary layer flow, shock wave configuration, density (and pressure) distribution, etc., particularly for simple shapes. Compared to conventional wind tunnel tests, the acquisition of data from range experiments requires much more effort and time. Nevertheless, because of some unique advantages, such as ability to obtain high relative velocities, high Mach and Reynolds numbers, freedom from interference, direct measurement of velocity and ambient conditions, ballistic range installations are in continuous use and development.

In order to fully exploit these advantages of range technique, particularly in relation to hypervelocity tests, it has been felt that a radically new approach to the instrumentation problem was required. The solution may be found in providing models with active instrumentation and telemetry to obtain the data from models in flight. In other words, miniaturization of standard free flight test technique is desired. A number of groups in the U.S.A. and in Canada are active in developing this technique.

The main difficulties to be overcome are the size of the transducer-telemeter system, which must be small enough to be accommodated in a model, and the requirement to withstand accelerations of several hundred thousand *g*. Preliminary results are encouraging in both respects.

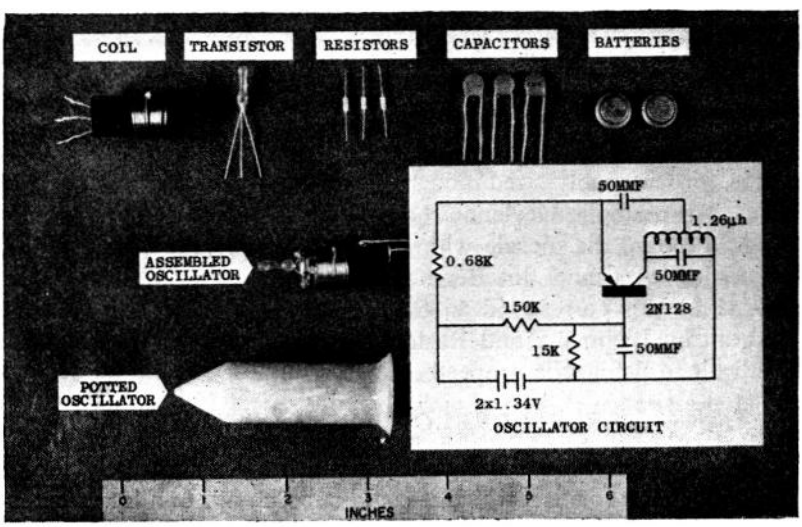

FIG. 36. Construction of the 20 mc oscillator.

The group at the Canadian Armament Research and Development Establishment, Quebec, succeeded in firing an artificially-modulated oscillator with a maximum acceleration of 10,000 g and is developing a multi-channel transmitter.

At the Gas Dynamics Facility, AEDC, a miniaturized 20 Mc oscillator was fired with initial accelerations of up to 200,000 g and its operation checked with several antennae spaced along the trajectory[42]. The oscillator circuit, its components and the assembled unit are shown in Fig. 36. All components, including batteries and transitor removed from its case, were potted in epoxy resin. The circuit was energized by joining with a drop of solder two wires which were brought to the surface. It was often possible to recover intact projectiles and to preserve the life of the batteries by disconnecting the circuit.

Further, efforts are being made to develop suitable receivers and miniaturized transducers which would be able to withstand high accelerations.

Electric-Arc Gun

The development of hypervelocity guns has been based, over the past ten years, on use of a propellant gas having a large velocity of sound. A number of gun designs, involving heating by combustion or by adiabatic compression of hydrogen and helium, have been evolved and small projectiles were accelerated to velocities up to about 15,000 ft/sec, compared to about 8000 ft/sec attainable with powder propellants.

At the AEDC, the electric-arc method of heating the air, already successfully used in hotshot tunnels, is being applied to development of hypervelocity guns, in the belief that much higher gas temperatures, and hence projectile velocities, can be obtained. The electric gun installation is shown schematically in Fig. 19, and the 0·55 in. electric-arc gun in Fig. 37.

So far, air has been heated in the arc-chamber of one of the hotshot tunnels to over 20,000°K. Hydrogen, initially at 35 atm pressure, has been heated to 2600 atm, corresponding to 14,000°K and over 90% monatomic hydrogen. It thus seems possible to obtain, by electric-arc heating, the ideal propellant.

The electric-arc heating is a constant volume process, so both the pressure and temperature of the gas increase drastically. Ideally, for a given amount of energy added, the final pressure is independent of density, whereas the final temperature is inversely proportional to it. Apparently then, the minimum feasible density of the propellant should be used for attainment of maximum muzzle velocity. In practice, account has to be taken of heat losses and efficiency of the heating process, so that an optimum density would be determined experimentally.

From the point of view of energy and propellant, it appears feasible to develop an electric-arc-driven gun with muzzle velocities of the order

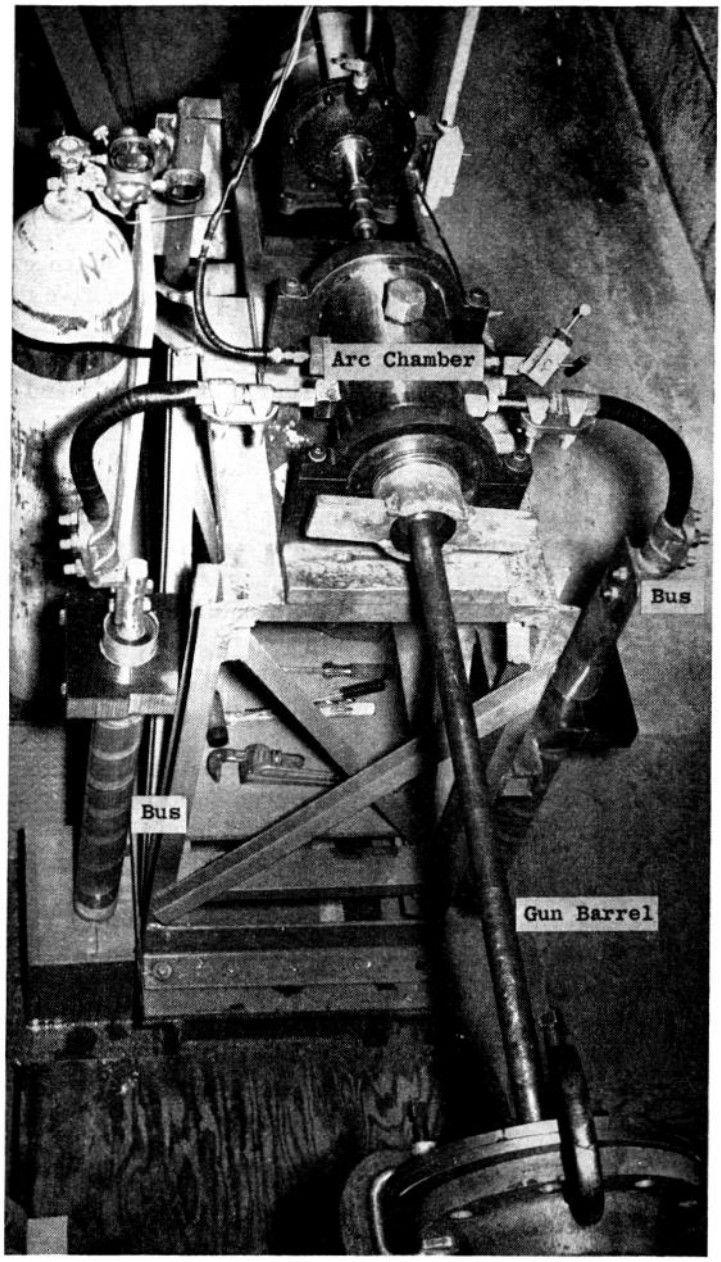

FIG. 37. 0·55 in. electric-arc gun.

of 30,000 to 40,000 ft/sec. However, many other design problems will require solution before a useful hypervelocity model launcher is developed. The erosion of gun barrels at the extreme gas temperatures is one of them and may require the use of an expendable barrel liner. The reduction of heat losses and of erosion might be eventually achieved by methods of magneto gas dynamics.

Trajectory Simulation

From the review of development of steady-state test facilities it is apparent that at present the provision of dynamic trajectory simulation would encounter serious difficulties and would be limited to velocities and densities small in relation to those encountered, for example, in some ballistic trajectories.

However, the simultaneous use of a hypervelocity gun and a supersonic nozzle, with the models launched upstream into the nozzle, offers the possibility, at least on a small scale, of trajectory simulation. This type of "entry simulator" is being developed since 1955 by Eggers at the NACA Ames Laboratory[43]. The atmospheric density distribution is simulated by a trumpet-shaped supersonic nozzle and models made of the same materials as the full-scale missiles are used. With this type of simulation the time scale of flight is greatly reduced, but heat transfer and thermal stress conditions are reproduced. From the observation of model in flight conclusions can be drawn as to the broad effects of entry into atmosphere on a full-scale missile.

9. FREE FLIGHT TESTING

It is apparent that ground-based test facilities are restricted as to the degree and type of simulation which they can provide. For this reason, the free flight test technique may be expected to play an increasingly important part in the investigation of hypervelocity flight. Moreover, it has the significant advantages of providing not only the actual ambient conditions but also a large model and time scale.

The presently-available technique of free flight testing may be regarded as a by-product of several years of growth of missile technology. As a result, certain propulsion and electronic components, which are produced in large numbers for military applications, may be used for free flight test vehicles. This is particularly significant in relation to the economy of this technique, which has been often considered too expensive to be practical.

The free flight test technique has been developed to a high degree of perfection by the NACA[43]. Propelled by multi-stage rockets, models were flown at Mach numbers of 10 and higher, and close control was exerted over the trajectories. For example, ballistic entry was simulated by using the final rocket stages to accelerate the model as it returned to the denser atmosphere.

The American full-scale experimental programme, culminating in the current X-15 spacecraft project, is an example of another type of free flight test.

Finally, one of the purposes of satellite experiments is to provide data in the flight regimes so far unattainable in ground test facilities.

10. CONCLUDING REMARKS

Following a decade in which only limited efforts were made to provide hypersonic and hypervelocity test facilities, we have, somewhat belatedly, entered a phase of vigorous development in this field.

As a result of introduction of high-temperature storage heaters and adoption of axi-symmetric nozzles, large hypersonic wind tunnels can be envisaged to provide velocity simulation up to Mach numbers of about 8 and Mach number simulation up to $M = 16$. The problem of throat design in two-dimensional, hypersonic nozzles—until recently, the road-block in the way of hypersonic tunnel development—has been eliminated by adoption of techniques akin to those successfully used for many years in the design of rocket nozzles: axi-symmetrical geometry and throat cooling by mass-transfer. The latter method of cooling is likely to undergo considerable development in the immediate future.

Conventional shock tubes are perhaps the exception in the field of hypervelocity test facilities, in that, being the ones first developed, they have already reached a high degree of perfection in a narrow, although important range of simulation, namely the simulation of aerodynamic heating in the stagnation regions of blunt bodies.

Attempts to develop shock tubes into hypervelocity wind tunnels have not been, so far, too successful, mainly on account of flow attenuation, short running times, and the attendant instrumentation difficulties.

In this respect, the development of electric-arc-driven hotshot wind tunnels has been more promising. Flow durations of up to one-twentieth of a second were obtained, and measurements of heat transfer rates, pressures and forces were made as in conventional tunnels. Moreover, with this technique relatively large densities and test sections are feasible. In the first, 16 in. dia. hotshot tunnel, conditions at 160,000 ft altitude and 15,000 ft/sec were simulated. The second hotshot tunnel has been built with a 50 in. dia. test section.

The electric-arc technique is only a recent development, as yet not fully explored. Further increase in the size of arc-driven installations may be expected, together with improvements in their design and in the quality of test data.

So far hypersonic wind tunnels have not been used for dynamic model tests, but there is no reason why this type of testing should not be undertaken in the future. Dynamic tests would be, however, rather difficult to perform in hypervelocity wind tunnels, because of the short running times available. The aeroballistic range and free flight techniques are

more suitable in this respect. The same is probably true of tests involving cooling by mass-transfer, such as film and oblation cooling.

The aeroballistic range technique has been, for many years, restricted to external observations of models and did not show much progress until very recently. We are now in the initial stages of development of instrumentation and telemetry for gun-launched models, and the early results are encouraging.

This is paralleled by development of hypervelocity guns. The application of electric-arc drive may offer means of reaching muzzle velocities not attainable with chemically-driven, light gas guns.

Apart from the launching phase, the instrumented model range technique is, in effect, a miniaturization of the free flight testing. Considerable progress has been made with the latter, including extension into the hypervelocity range. Since the trajectory conditions are most easily simulated with free flight technique, its usefulness is likely to increase as the speed increases.

The hypervelocity trajectories extend into the region of vanishingly small densities. Although for some 10 years now low-density, supersonic wind tunnels have been in operation, there is a fundamental difficulty in obtaining low-density equilibrium hypervelocity flow, due to the finite time rates of the kinetic processes involved.

Also, consideration of low-density, hypervelocity flows indicates that, because of the increase in density near the surface of a body, the phenomena associated with large mean free path would occur at much lower ambient densities than has been hitherto often supposed.

The aeroballistic range and free flight techniques, including the satellite experiments, may provide a solution to investigation of hypervelocity flight at extreme altitudes.

Acknowledgements. The author is indebted to the staff of the Gas Dynamics Facility, ARO, Inc., AEDC, for assistance in the preparation of this paper.

Thanks are due to Sandberg-Serrell Corporation, Pasadena, California, U.S.A., for permission to publish material presented in Figs. 12 and 15, and to the National Advisory Committee for Aeronautics, U.S.A., for the data on an electric air heater.

REFERENCES

1. P. R. Owen, Note on the Apparatus and Work of the WVA Supersonic Institute at Kochel, S. Germany, Royal Aircraft Establishment TN-AERO 1711, October 1945.
2. Julian H. Allen and A. J. Eggers, Jr., A Study of the Motion and Aerodynamic Heating of Missiles Entering the Earth's Atmosphere at High Supersonic Speeds, NACA-TN-4047, October 1957.
3. R. A. Minzner and W. S. Ripley, The ARDC Model Atmosphere, 1956, ARDC, USAF, ASTIA Document 110233.

4. JULIAN H. ALLEN, Hypersonic Flight and the Re-entry Problem, *J. Aero. Sci.*, Vol. 25, No. 4, p. 217, April 1958.
5. R. SMELT, Test Facilities for Ultra-High-Speed Aerodynamics, *Proceedings of the Conference on High-Speed Aeronautics*, Polytechnic Institute of Brooklyn, January 1955.
6. W. E. MOECKEL, Oblique Shock Relations at Hypersonic Speeds for Air in Chemical Equilibrium, NACA-TN-3895, January 1957.
7. HSIEN K. CHENG, Similitude of Hypersonic Flows over Thin and Slender Bodies—An Extension to Real Gases, CAL Report AD-1052-A-6, AFOSR-TN-58-87, AD-148 136, February 1958.
8. J. R. STALDER, A Survey of Heat Transfer Problems Encountered by Hypersonic Aircraft, *Jet Propulsion*, Vol. 27, No. 11, p. 1178, November 1957.
9. MAC C. ADAMS and R. F. PROBSTEIN, On the Validity of Continuum Theory for Satellite and Hypersonic Flight Problems at High Altitudes, *Jet Propulsion*, Vol. 28, No. 2, p. 86, February 1958.
10. H. S. TSIEN, Superaerodynamics, Mechanics of Rarefied Gases, *J. Aero. Sci.*, Vol. 13, No. 12, pp. 653–64, December 1946.
11. H. W. LIEPMANN and A. ROSHKO, *Elements of Gasdynamics*, J. Wiley and Sons Inc., 1957.
12. LESTER LEES, Recent Developments on Hypersonic Flow, *Jet Propulsion*, Vol. 27, No. 11, p. 1162, November 1957.
13. S. A. SCHAAF and S. F. SHERMAN, Skin Friction in Slip Flow, *J. Aero. Sci.*, Vol. 21, p. 85, February 1954.
14. K. N. C. BRAY, Departure from Dissociation Equilibrium in a Hypersonic Nozzle, British ARC 19983, March 1958.
15. J. D. LEE and G. L. VON ESCHEN, Preliminary Studies, Design and Theory for the Ohio State University Hypersonic Wind Tunnel, Technical Report No. 1, the Ohio State University Research Foundation, August 1956.
16. J. M. ALLEN, J. F. QUIRK, J. J. WARD and D. R. BRESSMAN, Determination of Preferred Method of Producing Air Temperatures Encountered in Flight by Hypersonic Aircraft and Missiles, AEDC-TR-57-11, July 1957.
17. P. E. PURSER and A. C. BOND, NACA Hypersonic Rocket and High-Temperature Jet Facilities, AGARD Report 140, July 1957.
18. A. FERRI *et al.*, Development of the Polytechnic Institute of Brooklyn Hypersonic Facility, WADC Technical Note 55–695, November 1955.
19. R. E. OLIVER and B. E. CUMMINGS, The Effect of a Simple Throat Distortion on the Flow in a Hypersonic Wind Tunnel Nozzle, *J. Aero. Sci.*, Vol. 24, No. 6, p. 466, June 1957.
20. C. H. MCLELLAN, T. W. WILLIAMS and I. E. BECKWITH, Investigation of the Flow Through a Single-Stage, Two-Dimensional Nozzle in the Langley 11-inch Hypersonic Tunnel, NACA-TN-2223, December 1950.
21. Aerodynamic Characteristics of Nozzles and Diffusers for Supersonic Wind Tunnels, Defense Research Laboratory, University of Texas, April 1951.
22. VIRGIL S. RITCHIE and RAY H. WRIGHT, and MARSHALL P. TULIN, An 8-foot Axi-symmetrical Fixed Nozzle for Subsonic Mach Numbers up to 0·99 and for a Supersonic Mach Number of 1·2, NACA-RM-L50A03a, February 1950.
23. S. A. SCHAAF, D. O. HORNING and E. D. KANE, Design and Initial Operation of a Low-Density Supersonic Wind Tunnel, University of California Report HE-150-62, August 1949.
24. BO K. O. LUNDBERG, Aeronautical Research in Sweden, *J. Roy. Aero. Soc.*, October 1955.
25. YING-NIEN YU, "A Summary of Design Techniques for Axisymmetric Hypersonic Wind Tunnels." AGARDograph (to be published).

26. M. H. Bloom and A. Pollone, Heat Transfer to Surfaces in the Neighborhood of Proturberances, 1957 Heat Transfer and Fluid Mechanics' Institute, Stanford University.
27. W. R. Thickstun, R. Schroth and R. Lee, The Development of an Axisymmetrical Nozzle for Mach 8, *Fourth U.S. Navy Symposium on Aeroballistics*, November 1957.
28. P. H. Rose, Physical Gas Dynamics Research at the AVCO Research Laboratory, AGARD Report No. 145, July 1957.
29. P. H. Rose and W. I. Stark, Stagnation Point Heat Transfer Measurements in Dissociated Air, *J. Aero. Sci.*, Vol. 25, No. 2, p. 86, February 1958.
30. J. A. Fay and F. R. Riddell, Theory of Stagnation Point Heat Transfer in Dissociated Air, *J. Aero. Sci.*, Vol. 25, No. 2, p. 73, February 1958.
31. E. Wittliff, M. R. Wilson and A. Hertzberg, The Tailored-Interface Hypersonic Shock Tunnel, Presented at ASME-ARS Aviation Conference, Dallas, Texas, March 1958.
32. A. J. Vitale, E. M. Kaegi, N. S. Diaconis and W. R. Warren, Results from Aerodynamic Studies of Blunt Bodies in Hypersonic Flows of Partially Dissociated Air, 1958 Heat Transfer and Fluid Mechanics Institute, University of California, Berkeley.
33. J. R. Stalder and A. Seiff, The Simulation and Measurement of Aerodynamic Heating at Supersonic and Hypersonic Mach Numbers, AGARD, June 1955.
34. R. N. Cox and D. F. T. Winter, The Light Gas Hypersonic Gun Tunnel at ARDC, Fort Halstead, Kent, AGARD Report No. 139, July 1957.
35. R. W. Perry and W. N. MacDermott, Development of the Spark-Heated, Hypervelocity, Blowdown Tunnel—Hotshot, AEDC-TR-58-6, June 1958.
36. J. Christopher Boison, Experimental Investigation of the Hemisphere Cylinder in Hypervelocities in Air, AEDC-TN-58-20, November 1958.
37. W. N. MacDermott, Preliminary Test Results With an Arc-Heated, Hypersonic Wind Tunnel at Mach Numbers of 10 to 20, Fifth Midwestern Conference on Fluid Mechanics, University of Michigan, April 1957.
38. R. R. Heldenfels and J. N. Kotanchik, Electric Arc-Powered Air Jets for Materials and Structures Testing at Temperatures to 10,000°R, National Summer Meeting, I.A.S., Los Angeles, July 1958.
39. R. L. Chuan and K. Krishnmutry, Principle and Application of the Two-Phase Wind-Tunnel System, USCEC Report 42-201, University of Southern California, December 1955.
40. G. J. Maslach and F. S. Sherman, Design and Testing of an Axi-symmetric Hypersonic Nozzle for a Low-Density Wind Tunnel, WADC Technical Report 56-341, August 1956.
41. F. M. Devienne, G. M. Forester and A. F. Roustan, Construction and Calibration of a Low-Density Wind Tunnel, Laboratoire Méditerranéen de Recherches Thermodynamiques, Nice, January 1958.
42. Stollenwerk and R. W. Perry, Preliminary Planning for a Hypervelocity Aeroballistic Range at AEDC, AEDC-TN-58-25, June 1958.
43. Forty-third Annual Report of the National Advisory Committee for Aeronautics, U.S. Government Printing Office, Washington 1957.
44. S. Feldman, Hypersonic Gas Dynamic Charts for Equilibrium Air AVCO Research Laboratory, 1957.

APPENDIX

Discussion of merits of two-dimensional and axi-symmetric nozzles, by A. Ferri *et al.*, p. 10, Ref. 18:

"Most existing hypersonic tunnels have used two-dimensional nozzles. This choice has been favored because the contoured walls can be made flexible and because the mounting of observation windows in the flat walls is simple. However, the two-dimensional nozzle has two fundamental disadvantages; first, the ratio between test section and throat areas increases so greatly with test Mach number that at Mach 10, for example, the throat height is about 1/500 of the test section height. This results in a slit-shaped throat area with a large wetted surface exposed to high rates of heat transfer and in a great sensitivity to local three-dimensional variations in slit height as may arise from thermal stresses or imperfections in fabrication. Second, the boundary layer on the flat walls of a two-dimensional nozzle is highly non-uniform because of the large transverse as well as longitudinal pressure gradients on those walls. As a result, it becomes increasingly difficult as the Mach number increases to correct for boundary layer effects by diverging the flat walls and/or adjusting the contoured walls.

"The axially-symmetric nozzle on the other hand has the optimum cross-sectional area at the throat from the point of view of wetted area and of sensitivity to thermal stresses. Thermal expansion at the throat does not introduce three-dimensional distortions and thus higher surface temperatures in the throat region can be permitted. Moreover, the boundary layer is also axially-symmetric and can be estimated with greater reliability than in the three-dimensional case. Thus, while the test section Mach number may change slightly with stagnation conditions because of boundary layer displacement effects, the flow distribution should remain unaffected thereby. The usual objections to axially-symmetric nozzles are that their Mach number cannot be varied; that the contoured surface must be very smooth in order to prevent large disturbances at the axis of the nozzle due to the focusing effect of internal cylindrical flow; and, finally, that it is difficult to install observation windows.

"For the hypersonic equipment at P.I.B. and for the types of tests to be run therein, the fixed Mach number feature of the axially-symmetric nozzle was not disadvantageous. Furthermore, for a test Mach number above 5, the disturbance caused by the window set tangent to the test section at the diameter normal to the windows is swept downstream at a small angle and thus does not affect a model. Finally, by making the nozzle long, that is, by making the maximum expansion angle small, it was thought that the focusing effect could be circumvented without impractically smooth contour walls. Moreover, several schemes of boundary layer control for effectively varying the nozzle contour have also been outlined and will be applied if necessary. It was thus decided to use axially-symmetric nozzles."